Alteration of Gold Nuggets Enriched with Platinum Group Elements (PGEs)

By: **Sophie E. Sperring**

A thesis submitted in partial fulfilment of the requirements of an Engineering Honours (BE(Hons)) in Chemical and Metallurgical Engineering Degree

Murdoch University, Western Australia

School of Engineering and Information Technology

December 2017

Word Count: 17, 260

Abstract

Understanding the mechanisms of incorporation, the form, and the solid-state solubility of Platinum Group Elements (PGEs) in gold nuggets at the nanoscale is critical to future works in gold (Au) nanoscale crystallography. Current works looking at similar samples include Mineral company research into extraction methods of similar samples and research in progress at the University of Western Austral using the alloy of the Au samples for medical purposes.

The work completed by this this used Au nugget samples that were taken from Ruby Creek, British Columbia, Canada. The geology specific to the Au samples used is a sub type of the placer alluvial is: Atlin gold placers, which are known for hosting a variety of metals, specific to the Atlin region.

Traditional thought for Au nuggets for monocrystalline structures. This steams from research completed by the minerals industry to extract the gold that lent into mineralogical studies. The gold rich rim consists of spherical particles that do not display the silver rich core parallel lamellae texture. The core structure is truncated where it meets the rim of the particle. No PGE particles within the sample area observed.

As seen with previous studies the Au samples display a rim that is silver (Ag) enriched. The rim could be a leaching mechanism experience by the gold in the presence of aqueous material. The relationship between the Au and the Ag was established as inversely proportional. The PGEs accumulated in the rounded, poly crystalline nanoparticulate Au-rich rim. The rim exhibited greater porosity within this rim area.

Majority of gain boundaries in the silver rich core of gold particles show a pile up of dislocations which result in multiplication of the diffraction maxima. The rim observed on the Au nugget samples were shown to have a PGE accumulation of between 10 to 20 μm.

The presence of the PGEs in solid solution is likely due to their relatively low concentrations and/or association with other trace elements such as Arsenic (As), Selenium (Se) and Sulphur (S), which may help to dissolve PGEs in the gold structure. The distribution seen of the PGEs suggests that during alteration of gold particles under supergene conditions, PGEs are subjected to the enrichment process due to a selective

dissolution of Ag. Homogeneous distribution of Ru, Rh and Pd in the gold matrix and lack of PGEs nanoparticles in the pores support this postulation.

The irrefutable evidence obtained from this study is that the PGEs are in solid solution in crystal structure in this sample. Exsolution does not occur at the nanoscale. It can also be said that during the process of alteration, the PGE accumulate in the Ag removed area.

The interest in this project will extend into Nano-SIMS academic activity to have a closer look at the isotopic complexity and to look at the distribution of isotopes of PGEs in gold sample. Looking for exsolution at absolute nanoscales and to see if the isotopes of the PGEs fractionate in the gold formation are also main features of the future work in this area of mineralogy.

Acknowledgements

This thesis submission acknowledges the financial support from School of Engineering and Information Technology, Murdoch University. The support from the faculty members; Dr. Malcolm P. Roberts, Dr. Aaron Dodd, and Dr. Alexandra Suvorova, and Dr. Martin Sounders at the Centre for Microscopy, Characterisation and Analysis, University of Western Australia is also acknowledged as invaluable. Finally, the ongoing support of supervisors to the project from Dr. Artur P. Deditius of The School of Engineering and Information Technology, Murdoch University and Dr.Fernando Barra of the Department of Geology and Andean Geothermal Center of Excellence (CEGA), Universidad de Chile, is appreciated greatly.

Contents

List of Figures

List of Tables

Chapter 1: Introduction

Deposits that contain gold have often been subjected to rigorous extraction due to the valuation of gold by society (Butt and Hough 2009). This value has scarcely evolved beyond a decorative element, but as technological advances continue, the value of gold is being placed in its nanoscale characteristics for biomedical and mechatronics applications. To utilise gold for economical and efficient extraction of gold for use in these applications reasons it is important to understand where the gold originates from, and the forms and associations it has with other elements during formation. Gold can form via either primary or secondary mechanisms.

Gold most often occurs at various areas of geomorphologic movement (Boyles 1979). Primary (hypogene) gold is gold that has been deposited from high-temperature hydrothermal fluids. Ore bodies that support gold formed from these systems, or the placers derived from them, are the most commonly mined deposits. Most primary gold consist of an alloy of Au and Ag, with the Au/Ag ratio >1. The gold typically contains 5–20 wt. % Ag, but in some deposits, it is essentially pure whereas, in others, the Ag content may exceed 50%.

1.1 Scope

The scope of this project was understanding and clarifying the mineralogical form of Platinum Group Elements (PGEs) at both a micro and nanoscale within gold nuggets from Ruby Creek, British Columbia, Canada. These samples have been generously supplied by Dr. Artur P. Deditius and Dr.Fernando Barra as part of a mineralogical series on the area. For this work, a set of microscopic techniques was utilized. The Ruby Creek deposit is a placer deposit often the source of gold, silver and PGEs samples due to the alluvial nature of the noble metal accumulation deposit (deposit of dense particles) (Hora, Pivec, and Langrova 2011, Mihalynuk et al. 2017). PGEs are a specific group of noble metals that display similar chemical and physical characteristics to one another. They include: platinum (Pt), palladium (Pd), osmium (Os), ruthenium (Ru), rhodium (Rh) and iridium (Ir). However, PGEs have a strong affinity towards

arsenic (As), sulphur (S), selenium (Se) and tellurium (Te) which result in complex mineralogy. So far, 144 minerals of PGE were identified (Smith and Nickel 2007).

There are two possible formations of these elements in gold: (i) solid solution and (ii) mineral nanoparticles separated from the Au structure. Complete solid solution can occur between the Au-Ag system. However, current binary diagrams between individual PGEs and Au (Ag) show no or very limited solid solution (Okamoto and Massalski 1984). In the presence of intermediate compounds such as the Au-Cu system; i.e. Auricupride (Cu_3Au) limited solid solution can occur with Au-Ag-PGE systems. Limited research has been completed in this area of mineralogy.

1.2 Objectives

This project attempts were made to elucidate the mechanisms of incorporation, the form, and the solid-state solubility of Platinum Group Elements (PGEs) in gold nuggets at the nanoscale. In addition, the fate of PGE during alteration of Ag-bearing gold nuggets were evaluated. This research is the foundation of multiple scientific papers, as part of a mineralogy series on the supplied Ag nugget samples.

Chapter 2: Literature review

The literature review incorporates strong elements of high level geology and mineralogy to assist in the understanding of the research completed. Too little work has been completed in this area of Nano mineralogy of gold geochemistry and crystallisation to analyse what has been completed and assess the gaps. This is the start of research in this area of mineralogy.

2.1 Types of Gold Deposits

Gold is often associated with a wide variety of minerals, with the highest occurring association being quartz, but this varies greatly on each individual deposit. Deposits of Au occur in the following time periods: Late Archean (for greenstone-hosted organic Au deposits), Paleoproterozoic (for iron oxide–copper–gold and lode gold deposits), and the Phanerozoic (for porphyry and epithermal deposits, Carlin-type Au deposits,) (Boyles 1979). Formation of gold deposits often corresponds with phases of new crustal growth, although these deposits are not necessarily at newly formed crustal areas (Sun et al. 2010).

Majority of gold containing deposits are porphyry deposits. They are formed from converging tectonic plates at subducting zones where the oceanic crust is depressed under the continental plate. This causes the upper mantle to melt partially and forces magmatic material to the surface. Fluidisation of the magmatic material disperses through various sized fissure areas. As the material cools, the metal precipitates from solution and migrates from the starting place. Typically, they are large with low grade dominant minerals associated with gold being Cu and Mo-bearing phases. These types of deposits contain ~20% of the world's gold (Palacios et al. 2001).

When formation occurs at lower temperatures to porphyry deposits, epithermal deposits occur. Deposits often have a combination of both formations within the regional area. Epithermal deposition is the formation from subaerial hydrothermal systems initiated by heat emanating from magmatic material and occasionally subterranean ground water at basin bounding faults (Tosdal, Dilles, and Cooke 2009). This deposition can be

subdivided into two groups based on mineralogical compositions: (1) quartz ± calcite ± adularia ± illite and (2) quartz + alunite ± pyrophyllite ± dickite ± kaolinite (Simmons, White, and John 2005). For group one the mineralogical composition is formed to the environmental conditions being at neutral pH and low sulphurisation to moderate sulphurisation (Sillitoe and Hedenquist 2003). Geothermal system is often volcanic rifting with meteoric water circulated within the zone (Tosdal, Dilles, and Cooke 2009). Deeper the water is generally chloride dominate with less of a sulphide content. The mineralogical composition of group two has formation that occurs in mid to high pH environments within largely sulphide based deposits (White and Hedenquist 1995); Although usually more associated with close surface magmatic-hydrothermal systems that are often highly acidic in nature (Tosdal, Dilles, and Cooke 2009). This type of deposit is potentially able to transport extremely large amounts of precious and base metals (Williams-Jones and Heinrich 2005). Despite the size of the deposits they are often formed within 1000s or even 100s of years. This is almost geologically instantaneous.

Both porphyry and epithermal deposits are sources for gold. Both instances have significant lithospherical geological profiles revolving around metamorphism in the mantle layer with hydrothermal fluidisation exolving oxidised magmatic material that penetrates the crustal layer where the physiochemical properties of the fluid cause precipitation of the precious and base metals. (Walshe and Cleverley 2009).

The continuum model (Phillips and Powell 2009) is used to attempt to understand Archaean gold forming deposits (Phillips and Powell 2009). Often this is the orogenic Au deposits (gold-only) and is a type of deposit that has formed over a 3-billion-year period (from as early as the Middle Archean in the Precambrian to the current day). Characteristics of the orogenic Au deposits are metamorphosed mid crustal blocks that are often deformed. (Goldfarb, Groves, and Gardoll 2001) such as the Archaean greenstone belts (Phillips and Powell 2009). The model projects that the hydrothermal Au deposits are formed at temperatures either above 700ºC or

below 180^{o}C, and in a 20-25 km upright, crustal profile. However, the continuum model however does not sufficiently cover why the orogenic Au formations occur as they do. These mechanisms of formation, although well documented, is not comprehended but the continuum model. Further research is still needed to understand formation of gold deposits at a mineralogical and geochemical level.

Post igneous formation of deposits, many are subjected to sedimentary processing to produce placer alluvial deposits. Majority of gold nuggets are formed in alluvial deposits and regions where the surrounding area is deeply weathered residual regolith as the gold erodes from the hosting rock and is transported, most often down streams and rivers (Hough, Butt, and Fischer-Bühner 2009). Previous work has found that the Au, Ag and Cu contents of alluvial gold grains in Chile could be traced to their potential host formation (Townley et al. 2003). Silver-rich (5 At %) grains with low Cu (0.1%) were found to come from epithermal systems and grains even richer in Ag (8%) but with low Cu (0.1%) were from Au-rich porphyries. Grains richer in Cu (up to 0.75%) with variable Ag contents, not surprisingly represented Au-rich Cu porphyries. Previous work found that alluvial gold grains in SW England contained appreciable Pd (3.1%), similar to the local primary mineralization (Chapman, Leake, and Moles 2000).

Clear geological understanding is the foundation of mineralogy. By understanding the origin and formation of the original samples and gold itself, estimations can be made on the mechanisms that produced the samples.

2.2 Deposition and Transport of Gold

Gold is effectively insoluble in water (Williams-Jones, Bowell, and Migdisov 2009) and commonly occurs in colloidal form. Colloids, are defined as the “particles that occupy the size range between true solutions and suspensions” (Eby 2016). In this form, Au precipitates in its physio-chemical properties. Au’s furthest outer electron cloud is readily delocalised because of weak bonding between individual Au ions (Eby 2016). This

causes formation of small Au clusters with charged outer surfaces (usually negative) that repeal each other to form colloids (collections of gold nanoscale particles) (Cobley and Xia 2009). This phenomenon frequently occurs during abrupt decrease of temperature that causes precipitation of gold. This suggests that colloidal gold may remain in suspension for extended periods. As such, it can be transported in low temperature environments, often accompanied by super saturation and polymerization of silica (Eby 2016).

Due to gold being a noble metal, it is less to almost no reactive at the surface when in contact with aquatic/aqueous environments as well as sulphide and chloride depleted gases. This causes gold to commonly occur in its native form. Gold dissolution and deposition is controlled by a hydrogen / sulphide / oxygen reaction at temperatures up to 350^{o}C and can be promoted by decreasing the activities of the other species and increasing the pH of the reaction (Hough, Butt, and Fischer-Bühner 2009). Sulphidation of wall rock is a process that can decrease the sulphur content of the mineralizing fluid. The sulphurisation of hosting iron mineral rocks occurs for example can cause the sulphur in solution with gold is significantly reduced. This is often why gold deposits are found in very close proximately to iron sulphides.

The oxidation reaction reduces the activity of the oxygen species that causes the Au precipitation to be minimalised as Au solubility in solution is increased. This oxidation could occur through interaction of the ore-bearing fluid with a hematite-bearing host rock or mixing with oxygenated meteoric water (Hough, Butt, and Fischer-Bühner 2009). Lastly the deposition of gold (e.g. As dendrites in amorphous silica) that occurs as a result of flocculation due to changes in the fluid chemistry. Such as increases in salinity or pH, both of which may occur as a result of boiling or fluid mixing (Williams-Jones, Bowell, and Migdisov 2009).

2.3 Content of PGEs in Gold Geology

Some Au/Ag deposits contain PGEs in the form of platinum group minerals (elements being distinctly different to mineralogical compounds (minerals)). One geological instance of this is in Catalonia, Spain within sulphide-rich shales that are closely linked to arsenic (Canet et al. 2003). These PGE minerals are found for: platinum, as sperrylite ($PtAs_2$), and palladium, as Pd-bearing löllingite $(FePd)As_2$, although native palladium and stibiopalladinite, Pd_5Sb_2 can also be found in small quantities (Canet et al. 2003).

Other deposits, such as volcanogenic massive sulphides (VMS), also contain minor quantities of PGEs. Specifically, Pt (188 ppb), Pd (318 ppb) and Rh (21 ppb), in selective areas of the Uzelginsk Deposit, Russia (Vikentyev et al. 2004). Under SEM this sample exhibited actual grains of native rhenium within the Au/Ag area of formation. Also seen within this deposit is a relationship between the Au/Ag content (Au at 1.8 ppm and Ag at 35 ppm). The Au and Ag proportionally increase with each other throughout the sample, and were uniformly distributed across the micro scale samples examined (20 -50 µm scales) (Vikentyev et al. 2004). Authors suggested that mineralogical features, i.e. presence of PGEs, tellurides and arsenides, implies precipitation of PGEs from Te and As rich hydrothermal solutions (Vikentyev et al. 2004). This can then lead to an enrichment of PGE in the mineralogy of the sample even in environments that are unsaturated in PGE.

2.4 Gold and PGE Crystallography

Previous work completed at a microscale on gold nuggets suggest a monocrystalline structure using EBSD to establish that the crystallographic orientation has no variation to it (Kikuchi – See Fig.1) (Hough et al. 2007). Kikuchi lines are used to diagnose monocrystalline structure but at a large scale. It was perceived that there was no nucleation of new grains within the core of the sample (Fairbrother et al. 2012).

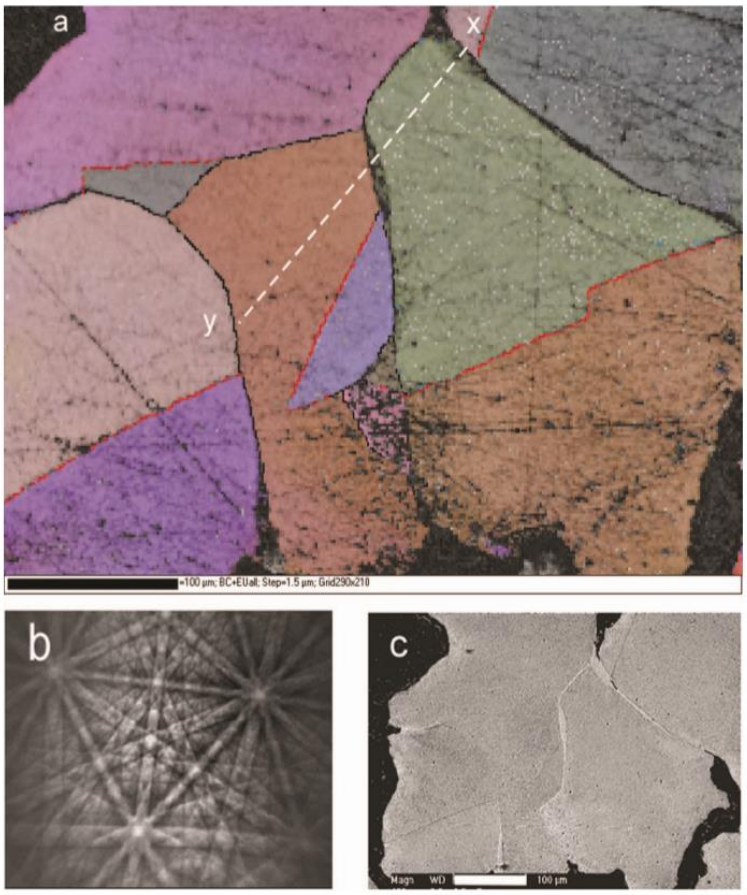

Fig.1: (a) Monocrystalline: Black lines mark grain boundaries and the red lines are twin planes 60° (111). X–Y marks location of electron microprobe transect; (b) Kikuchi lines obtained during orientation mapping of sample; (c) Atomic number contrast image of area mapped in (a) showing bright zones at grain boundaries representative of Ag depletion in the alloy. (Hough et al. 2007).

Most often to understand relationships of native gold with other elements occurring in native form is to study their crystal-chemical properties. Table 1 summarizes structural properties of Au and PGEs. With the exceptions of Rh and Os, the crystal structure of all minerals is isometric hexoctahedral. All the elements of interest occur within the same region of the periodic table. One of the possible approaches is to investigate crystal-chemistry of Au and metals as a function of temperature using binary and ternary diagrams.

The best known binary system is Au-Ag (White, Orr, and Hultgren 1957, Dowdell et al. 1943). However, there is a limited amount of information on Au-platinum group elements (PGE) relation. Fig. 1 shows an Au-Ag-Cu system that attempts to provide a framework for a discussion of the formation of these rare alloy compositions (Knight and Leitch 2001).

It is near impossible to replicate synthetically the equilibrium of Au alloys. The (Knight and Leitch 2001) research studied over 80 samples of naturally occuring Au-Ag-Cu nuggets to determine the percentages needed to estimate the system (Fig. 1).

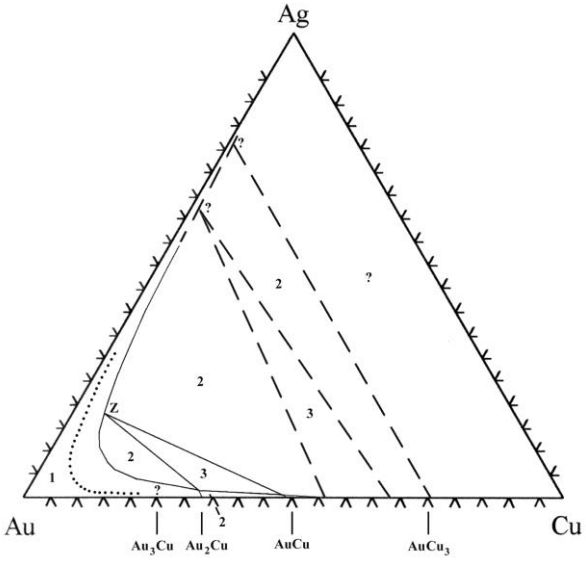

Figure 2. Phase diagram in Au-Cu-Ag system at temperature less than 100ºC (Knight and Leitch 2001)

Table 1: Crystallographic information of Au, Ag, and PGE

Element	Cell Dimensions	Crystal System	X-ray Diffraction
Au	A = 4.0786, Z = 4; V = 67.85 Den(Calc)= 19.28	Isometric - Hexoctahedral H-M Symbol (4/m 3 2/m) Space Group: F m3m	By Intensity(I/I_o): 2.355(1), 2.039(0.52), 1.23(0.36),
Ag	A = 4.0862, Z = 4;V = 68.23 Den(Calc)= 10.50	Isometric - Hexoctahedral H-M Symbol (4/m 3 2/m) Space Group: F m3m	By Intensity(I/I_o): 2.359(1), 2.044(0.4), 1.231(0.26),
Pt	A = 3.9231, Z = 4;V = 60.38 Den(Calc)= 21.46	Isometric - Hexoctahedral H-M Symbol (4/m 3 2/m) Space Group: F m3m	By Intensity(I/I_o): 2.265(1), 1.962(0.53), 1.1826(0.33),
Pd	A = 3.8824, Z = 4; V = 58.52 Den(Calc)= 12.19	Isometric - Hexoctahedral H-M Symbol (4/m 3 2/m) Space Group: F m3m	By Intensity(I/I_o): 2.246(1), 1.945(0.42), 1.376(0.25),
Ru	A = 2.704, c = 4.326, Z = 2; V = 27.39 Den(Calc)= 16.65	Hexagonal – Dihexagonal Dipyramidal H-M Symbol (6/m 2/m 2/m) Space Group: P	By Intensity(I/I_o): 2.056(1), 2.343(0.4), 2.142(0.35),
Rh	A = 3.856, Z = 4; V = 57.33 Den(Calc)= 14.59	Isometric – Hexoctahedral H-M Symbol (4/m 3 2/m) Space Group: F m3m	By Intensity(I/I_o): 0.7874(1), 0.8623(0.8), 0.8847(0.7),
Os	A = 2.714, c = 4.314, Z = 2; V = 27.52 Den(Calc)= 23.01	Hexagonal – Dihexagonal Dipyramidal H-M Symbol (6/m 2/m 2/m) Space Group: P 6_3/mmc	By Intensity(I/I_o): 1.22(1), 2.13(1), 1.35(0.6),
Ir	A = 3.8394, Z = 4; V = 56.60 Den(Calc)= 21.45	Isometric - Hexoctahedral H-M Symbol (4/m 3 2/m) Space Group: F m3m	By Intensity(I/I_o): 2.217(1), 1.9197(0.5), 1.1574(0.45),

The system takes into account limits set on exsolution growth from the study by (Murzin et al. 1983) for the concentrations of Ag in Au–Cu alloy and the amount of Cu in Au–Ag alloy beyond which exsolution occurs. Within the study the sample values for Cu in Au–Ag alloy are below 100°C and the Cu practically non-existent in other samples (Knight and Leitch 2001). However, in cases of extremely low Cu content were not used in the diagram created (Figure 3).

2.5 Miscibility in Au-Ag-PGE system

A published phase diagram for Au-Ag-PGE systems does not exist in published literature. The diagram created for this document in Fig. 2 is an accumulation of published work done on gold samples that contain Ag (0-63%) and the PGEs, Pt and Pd (0-15% cumulatively) set as weight percent. There is a very limited amount of information on this particular ternary system. However, one early conclusion is derived from the similarity to Fig.1, is the ratios of Au-Ag-Cu being very similar to the Au-Ag-(Pt+Pd).

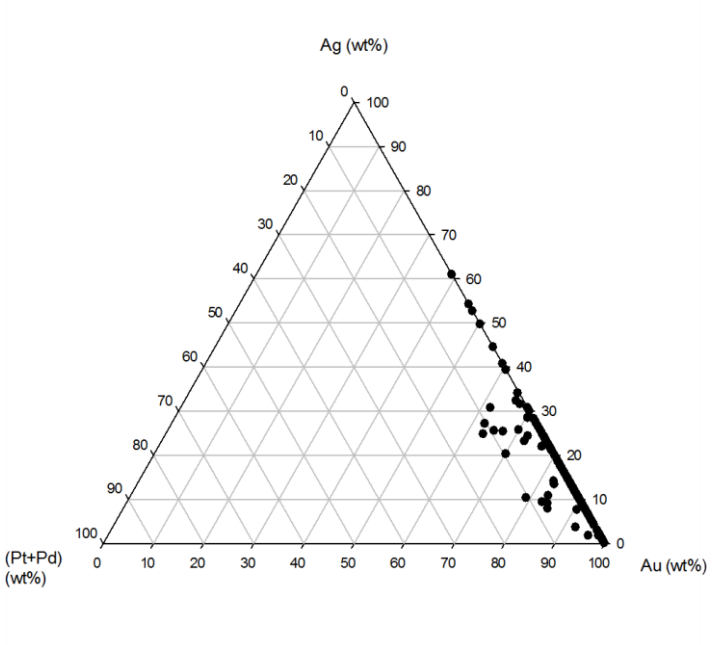

Figure 3: Phase diagram in Au-Ag-(Pt+Pd) system from literature.(174 separate articles listed in refernces)

There has been efforts to understand through phase diagrams of various binary Au systems with singular PGEs, such as in (Okamoto and Massalski 1984) where the diagram between Au and Os was attempted. In (Guha 1985) there are binary systems of Au-Pt, Au-Pd, and Au-Rh (see Figure ##). These binary systems exist at high temperature ranges (600 -2200ºC) with large exclusion zones of formation where high percentages of PGE were unlikely to occur below the higher temperature range (>1500ºC) (Guha 1985).

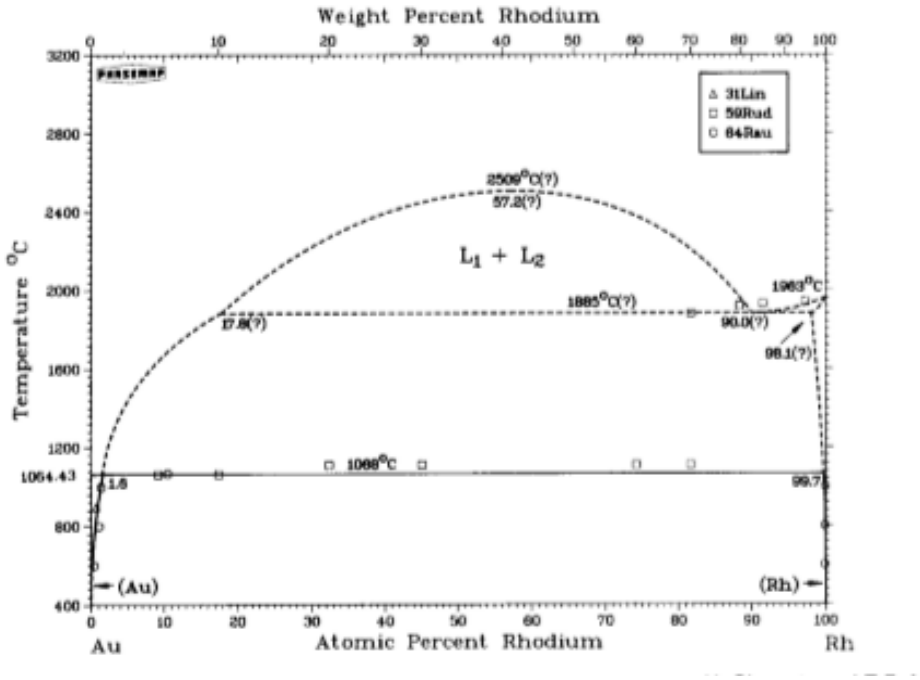

Figure 4: Binary System of Au and Rh (Guha 1985).

2.6 Alteration of Au Nuggets – Previous literature on Ag Depleted Rims

Previously mentioned, Au and Ag are geologically commonly associated. This is only currently confirmed at the macro scale. Both Au and Ag have the same atomic radius and crystal systems, so they can form a continuous alloy series (See Table 1). When the Ag content exceeds 20 wt.%, the alloy is termed electrum (Hough, Butt, and Fischer-Bühner 2009). It was noted that gold nuggets altered under near-surface conditions exhibit the core rim texture. Rimming is a common feature on gold nuggets enriched with Ag and being exposed to weathering under Earth surface conditions; i.e. critical zone.

The external layer of Au nuggets are usually a few microns thick, is enriched with Au and depleted in Ag and other metals if present (Groen, Craig, and Rimstidt 1990). In the instance of Ag depletion, the structure of gold rim has a lack of inclusions of Ag. The boundary between Ag-rich and Ag-depleted areas follows distinctive crystal boundaries. This suggests that silver depletion is a result of interaction with altering fluids (Aqueous based) than dissolution and re-precipitation of Au.

This depletion is cause by preferential leaching of the silver in alluvial settings. This is because the silver is more readably soluble than Au (Hough et al. 2007). Although the crystalline nature of the grains specifically is limited, it justifies the observation of the internal veining of the material. However, there is a limited knowledge on the geochemical behaviour of PGEs during alteration of Au nuggets.

For example, the Kondyor PGE placer deposit, Khabarovskiy Kray, Russia is one deposit that exhibits a gold-rich rim, with four groups of gold alloy present: tetra-auricupride, Au–Ag ratio (98–54 wt. % Au, to relevant Ag %), Au–Ag–Cu–Pd and Au–Pd–Cu alloys (Shcheka et al. 2004). The inner portion contains a host of PGE elements with a proportionally different Au/Ag ratio. Although shown to exist, the focus of the paper remained on macro crystals of Pt-Fe alloys over Au/Ag ratios or the Au rich rim itself.

Studied samples from Ruby and Wright creeks (BC, CAD) display a similar rim pattern that is linked to the depletion of Ag, Hg and Cu from the gold nuggets. This is displayed within the sample as small pitting (Hora, Pivec, and Langrova 2011). For Atlin gold samples the rims are linked to the identified bedrock source in Klondike District, Yukon (Knight, Morison, and Mortensen 1999).

2.7 Mobilisation of Gold

Under surface conditions, gold occurs in aqueous solution in colloidal form [Au(0)] and in aurous [Au(I)] and auric [Au(III)] complexes; the standard

reduction/ oxidation potentials of Au+ (1.68 V) and Au^{3+} (1.50 V) exceed that of water (1.23 V), which makes the sustainability of free gold ions thermodynamically unfavourable (Boyles 1979) (Southam et al. 2009). This Ag depleted rim could to be due to supergene gold mobility within a thiosulphate complex under alkaline to neutral pH.

In this instance, the thiosulphate is attached to the flexible extended chain of a humic acid as smaller molecules. A humic substance is a type "of naturally occurring, biogenic heterogeneous organic substance that can generally be categorised as being ... of high molecular weight and refractory" (Eby 2016, Groen, Craig, and Rimstidt 1990). Specifically, a humic acid is a humic substance that is soluble in water at pH greater than 2. Humic acids in the presence of dense vegetation allow for Au mobility in subsurface waters. This mobility can affect older Au grains, detrital organics or newly formed iron sulphides (Eyles and Kocsis 1988, Eyles 1990, Groen, Craig, and Rimstidt 1990, Bakos et al. 2004).

Bacteria can also be a mechanism of metallic mobility. The metallophillic bacteria Cupriavidus *metallidurans* CH34 (C. *Metallidurans*) is able to biomineralise Au nanoparticles due to an Au-regulated gene that causes energy dependent reductive precipitation of Au (III) auric complexes. (Reith et al. 2009). These bacteria are essential to biogeochemical recycling of Au, PGEs and other precious metals that share geochemical properties similar to Au (Rauch and Morrison 2008). This nanoscale bacterial mobility could also be a factor in the gold rim formation

Bacterial Biofilms associated with the Ralstonia *metallidurans* show an aerated network of budding spherical particles as small as 3 µm (Reith et al. 2006).

Chapter 3: Analytical Methods

Scanning Electron Microscopy imaging and elemental mapping was completed on the FEI Verios 460 SEM. Compositional analyses were acquired on a JEOL 8530F electron microprobe equipped with five tuneable wavelength dispersive spectrometers.

Operating conditions were 40 degrees take-off angle, an electron beam energy of 25 kev, and a 40 na beam current. The beam was fully focussed. Elements were acquired using analysing crystals lif for Fe Kα, Au Lα, Te Lα, Cu Kα, Ni Kα, Co Kα, Cr Kα, Hg Lα, Re Lα, Os Lα, Ir Lα, Pt Lα, V Kα, Mn Kα, PETH for Pb Mα, Sb Lα, Bi Mα, Ti Kα, PETJ for S Kα, Ag Lα, Pd Lα, Ru Lα, Rh Lα, and TAP for As Lα, Se Lα and Si Kα.

The standards used for X-ray intensity calibration were a selection of elements, synthetic and natural minerals: synthetic Cr_2O_3 for Cr Kα, galena for Pb Mα, S Kα, pyrite for Fe Kα, rutile for Ti Kα, Bi_2Se_3 for Se Lα, Ag for Ag Kα, Cu for Cu Kα, Ni for Ni Kα, V for V Kα, wollastonite for Si Kα, Co for Co Kα, Bi for Bi Mα, Pt for Pt Lα, Sb for Sb Lα, arsenopyrite (Asp200) for As Lα, Mn for Mn Kα, Au for Au Lα, Ru for Ru Lα, Rh for Rh Lα, Pd for Pd Lα, Os for Os Lα, Ir for Ir Lα, Re for Re Lα, Te metal for Te Lα, and synthetic hgte (coloradoite) for Hg Lα.

The on-peak counting time was 20 seconds for V Kα, Mn Kα, Ti Kα, and 30 seconds for Fe Kα, Se Lα, Au Lα, Te Lα, Cu Kα, Pb Mα, Ni Kα, Co Kα, Ag Lα, Bi Mα, Si Kα, Pd Lα, Ru Lα, Rh Lα, Cr Kα, Hg Lα, Re Lα, Os Lα, Ir Lα, Pt Lα, S Kα, As Lα, Sb Lα. Mean atomic number (MAN) background intensity was used throughout (Donovan and Tingle 1996, Donovan, Singer, and Armstrong 2016).

Unknown and standard intensities were corrected for deadtime. Interference corrections were applied to S for interference by Co, and to As for interference by Sb, and to Sb for interference by Bi, and to Fe for interference by Pb, and to Se for interference by As, Co, and to Te for interference by Co, and to Bi for interference by S (Donovan, Snyder, and Rivers 1992). The matrix correction method was the ZAF algorithm of Armstrong/Love Scott (Armstrong 1988)

The thin-foil were cut perpendicular to the boundary between Au-rich rim and Ag-rich core. Samples were prepared by using FEI Helios nanolab G3 CX dualbeam and focused ion beam (FIB) at CMCA in UWA. Sections were extracted from the sample surface by in-situ lift-out, welded onto a copper grid, thinned to electron transparency with a 30kv ion beam where the beam current was progressively reduced from 2.5na to 0.23na, and then finally polished with a 5kv beam with a 41pa current (See appendix 1 through 3). Subsequently, the samples were analysed by using a Titan G2 80-2090 TEM/STEM with chemistem technology at 200kv.

Chapter 4: Results

4.1 Location and Description of Samples

The geology specific to the Au samples used is a sub type of the placer alluvial is Atlin gold placers, which are known for hosting a variety of metals, specific to the Atlin region. The Atlin region consists of sedimentary material formed from Mississippian to Jurassic age, and ophiolitie of Late Permian to Triassic age, and Middle Jurassic, Cretaceous and Tertiary igneous rock (Hora, Pivec, and Langrova 2011). Although the ages are various, the Atlin area has dales that score the native bedrock and have become modified to support glacial and glaciofluvial deposits (Levson et al. 2003). Bedrock that hosted the gold that supplies the Atlin region is majority unknown. However, a distinctive pattern of placer streams on every side of surprise lake batholiths exists, with the coarse gold particles found within streams that run along the margin.

The gold particles have rounded or flaky morphology with maximum dimension of 1 cm. The back scattered electron (BSE observations show a rim-core texture of variable thickness from few to ~ 100 µm (Fig. 4 (a)). The rim is composed of two different zones: (i) brightest in BSE, 10-80 µm thick inner zone containing relatively large pores, 10-20 µm in diameter; and (ii) darker in BSE (same grey level as the core in BSE), ~10 µm thick outer zone containing numerous and smaller pores < 5 µm in diameter.

4.2 Paragenisis and Composition

As previously mentioned, all three samples tested were Au nuggets with silver inclusions. The gold content across the sample is lowest at 74 wt. % up to 98.9 wt. %. The Ag content across the sample also had a large range between 0.5 wt. % to 26 wt. %. The microprobe analysis establishes that the PGEs exist in variable quantities in the sample. (Full microprobe data can be seen in Appendix 3). The PGE percentage is approximately 0.5 wt. % to 1.4 wt. % across the sample. Other elements are shown to be present in the sample in small percentages (maximum content given): Se (2.5 wt. %), As (2.3 wt. %), Hg (1.3

wt. %) Fe (0.8 wt. %), Bi (0.6 wt. %), Si (0.5 wt. %) Pb (0.4 wt. %), and S (0.4 wt. %). Smaller inclusions of Ti, V and Mn exist above detection limits.

Surrounding the sample is mineralogy that is encased in the boundaries. The compositions of these minerals (Appendix 1) suggest the area is comprised of mostly feldspars (primarily orthoclase but some plagioclase varieties are also present), quartz, biotite, chlorites, hornblende and possibly garnet group minerals. These estimations are from chemical breakdowns in Fig.10. There is an arbitrary cohesion of the minerals in the edge of the sample (Fig.5a). Au inclusions can be seen speckled in the sample as seen in (Fig.5b).

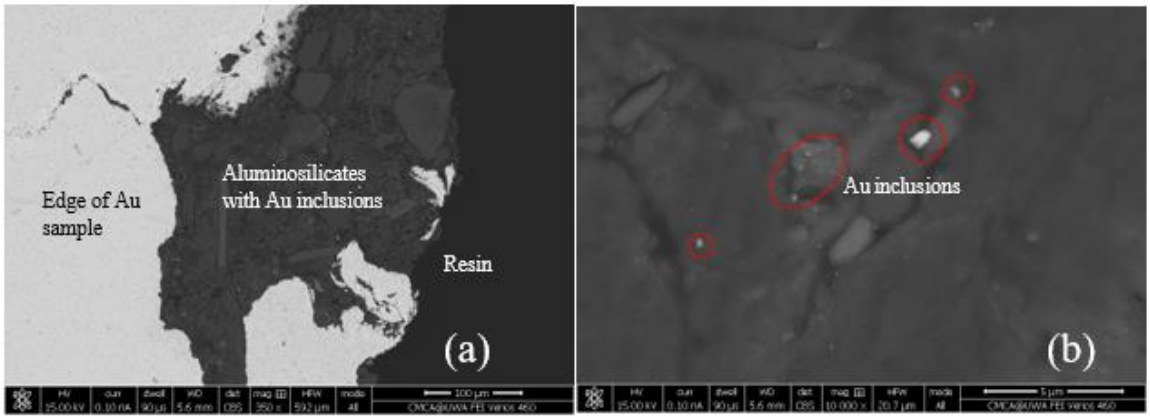

Figure 5: (a) Edge of the gold particle with aluminosilicates; (b) Gold particles in the silicate matrix is highlighted in the red.

4.3 Silver Depleted Rim

The texture of the Au nugget is simplistic under the SEM imaging. As seen from previous studies the Au samples display a rim that is Au enriched. The rim is a sign of either a leaching mechanism experience by the gold in the presence of aqueous material composed of Cl, Br and SO_4 or other biogeological mechanisms. This area extends between 2-20 microns thick.

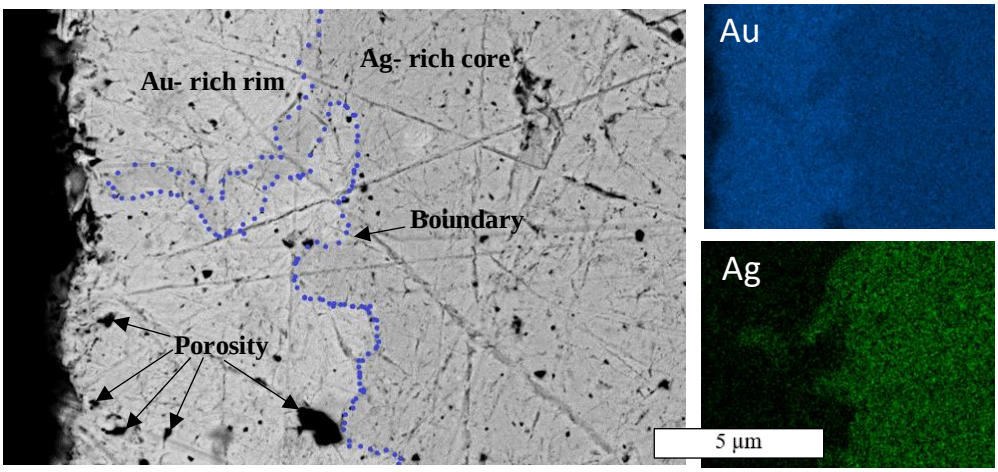

Figure 6. Boundary between Ag depleted rim and Ag rich core (blue dotted line) associated with EDS elemental Maps.

Around the edge there is noticeable deterioration within the porous area that are less frequently seen in the core. The distinctive rim is brighter on the edge due to the higher percentage of Au in this area (Fig. 6) (Fig.7a).

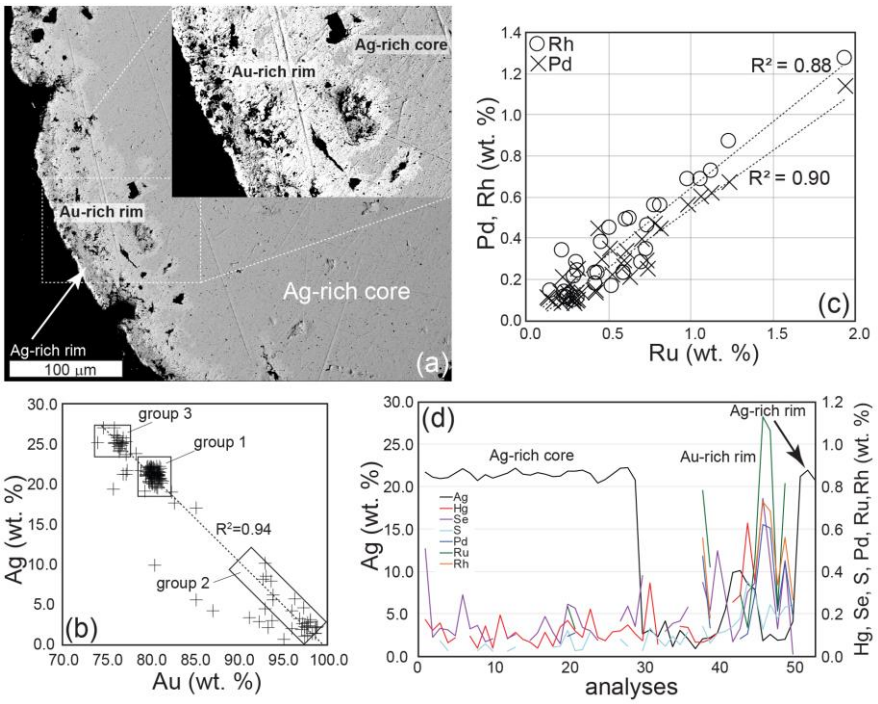

Figure 7. (a) Back-scattered electron (BSE) image of gold nugget and rim area (inset). Note the alternate sequence of Ag-rich core, Au-rich rim, and Ag-rich rim. Porosity in rim; (b) Plot of Ag vs. Au showing variation of the chemical composition of Au nuggets (groups 1, 2, and 3); (c) Plot showing and positive correlation of Pd and Rh vs. Ru; (d) EPMA traverse through the rim of Au nugget. Note the increase in the concentration of Pd, Rh, Ru, Se, S and Hg towards the in rim of nugget.

The relationship between the Au and the Ag is inversely proportional (Fig.7b). The graph shows three distinct areas with two different cores (groups 1 and 3) and the combined rim.

Group 1 is a tightly packed area and expresses a 20-22% Ag content with 78-80% Au. As the core makes up majority of the sample, this collection represents this area. The concentration is dense as the core is crystalline growth that are regular in composition. The lack of external interaction means the zone is analogous in composition.

Group 2 is a cluster that is comprised of the rim of the samples. The Au is proportionally high (90-99%) compared to the Ag content (0-5%). The scattering in this group is due to the variability of the Ag removal from the rim and subsequent replacement of Au in this area. This inconsistency leads to greater unpredictability in this group. Despite this, both rims from each sample fall in this group.

Group 3 is comprised of 22-25% Ag with only 75% Au. This core has a greater silver content than the other core sample. The PGE elements appear to form with each other within the sample. Positive liner correlation exists with Pd and Rh when associated with the Ru (dominant PGE) (Fig.7c).

The data from the EPMA traverse in (Fig. 7d) indicates the percentage relationship between the Au and the Ag is negatively correlation with the core having an estimated average of 22-23% Ag and only 2-3% within the rim. The PGE data that exists above the detectable limit seem to concentrate around where the Ag is lower in concentration with the Ag trough at analysis 47 showing peaks of Pd, Rh and Ru especially. The Au sample has various areas of porous zones residing in both the core and the rim (see Fig. 7a). Most of the porous area is seen along the Ag depleted rim. These areas are viable as potential areas of reactivity with environmental exposure. Majority of pores are in the rim and increases towards to rim of the nuggets (Fig. 7a).

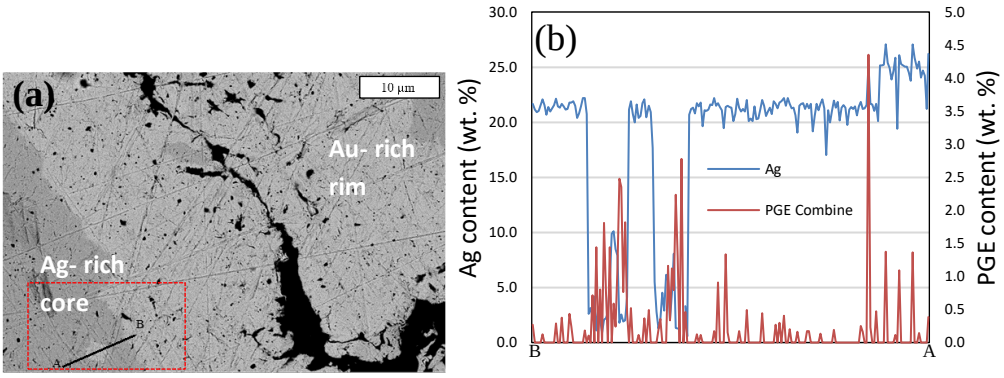

Figure 8. (a) Change in the relative concentration of Ag & PGE along traverse, "A" to "B"; (b) Graph of concentration.

A section of sample was examined for both Ag and PGE elements from points A to B (Fig. 8a). The data shows a relationship between the Ag and PGE. As the Ag is removed from the sample in the lighter areas, the PGE content increases in those areas (Fig. 8b).

4.4 Structure and Composition of Gold at the Nanoscale

The structure of the sample produced a different image than expected. Traditional thought is at the microscale (then presumably the nanoscale) Au nuggets for monocrystalline structures. The gold rich rim consists of spherical particles that do not display the silver rich core parallel lamellae texture. The core structure is truncated where it meets the rim of the particle (Fig. 9a). The rim is of variable size up to 1 micron, core individual lamellae 50 – 700 nm separated into nanodomains caused by strain. There is a lack of porosity passing from rim to core during TEM.

Elemental maps make the distinction clearer with the Ag absent in the rim. The composition of this sample did not have Pd in high enough quantity to be detected by instrumentation, however the Ru was above the detection limit. The Ru appears homogeneous across the entire sample (core and rim)sample with no distinctive particles of Ru (or any PGE) in the elemental maps. Higher energy ranges were used to see peaks of the PGE material that usually overlaps with

both Au and Ag at lower ranges. The peak of Ru Kα that is separate from the later peaks of Ag Kα and Kβ (Fig. 9b).

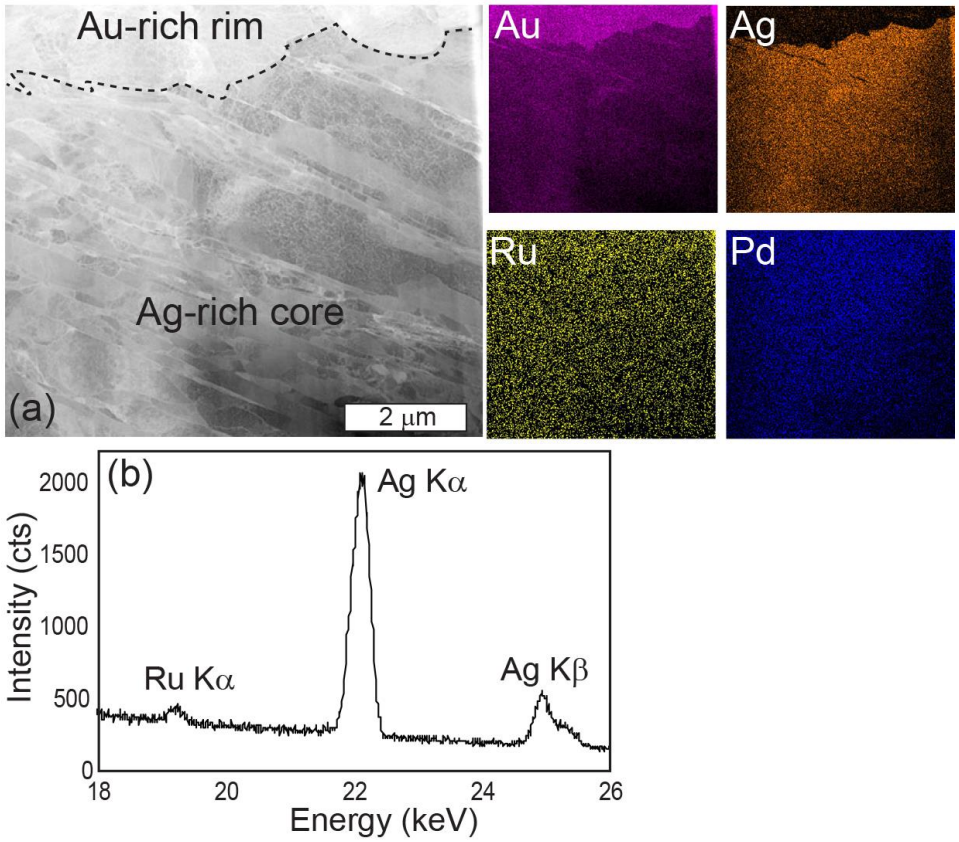

Figure 9. (a): HAADF-STEM image of the contact between Au-rich rim and Ag-rich core associated with TEM-EDS elemental mappings. Note: core structure is truncated where it meets the rim of the particle, core individual lamellae 50 – 700 nm separated into nanodomains caused by strain, lack of porosity in TEM: (i) inverse relationship between Au and Ag; and (ii) homogeneous distribution of Ru and Pd, which document lack of (Ru, Pd) nanoparticles; (b) Fragment of the EDS spectrum of documenting presence of Ru in the matrix of Au nuggets.

It can be observed in the Ag rich core a polycrystalline lamellae structures (Fig. 10a). No PGE particles within the sample area observed. Sometimes the grain boundary between the individual lamellae is irregular in shape which resembles or suggest corrosion or dissolution process. However close examination revealed that this irregular boundary is a single crystal of gold with accumulated stain (Fig. 10c).

FFT analysis of the HR-TEM image revealed the presence of twinning between individual lamellae of gold (Fig. 10d). Majority of gain boundaries in the silver

rich core of gold particles show a pile up of dislocations which result in multiplication of the diffraction maxima (Fig. 10e and f).

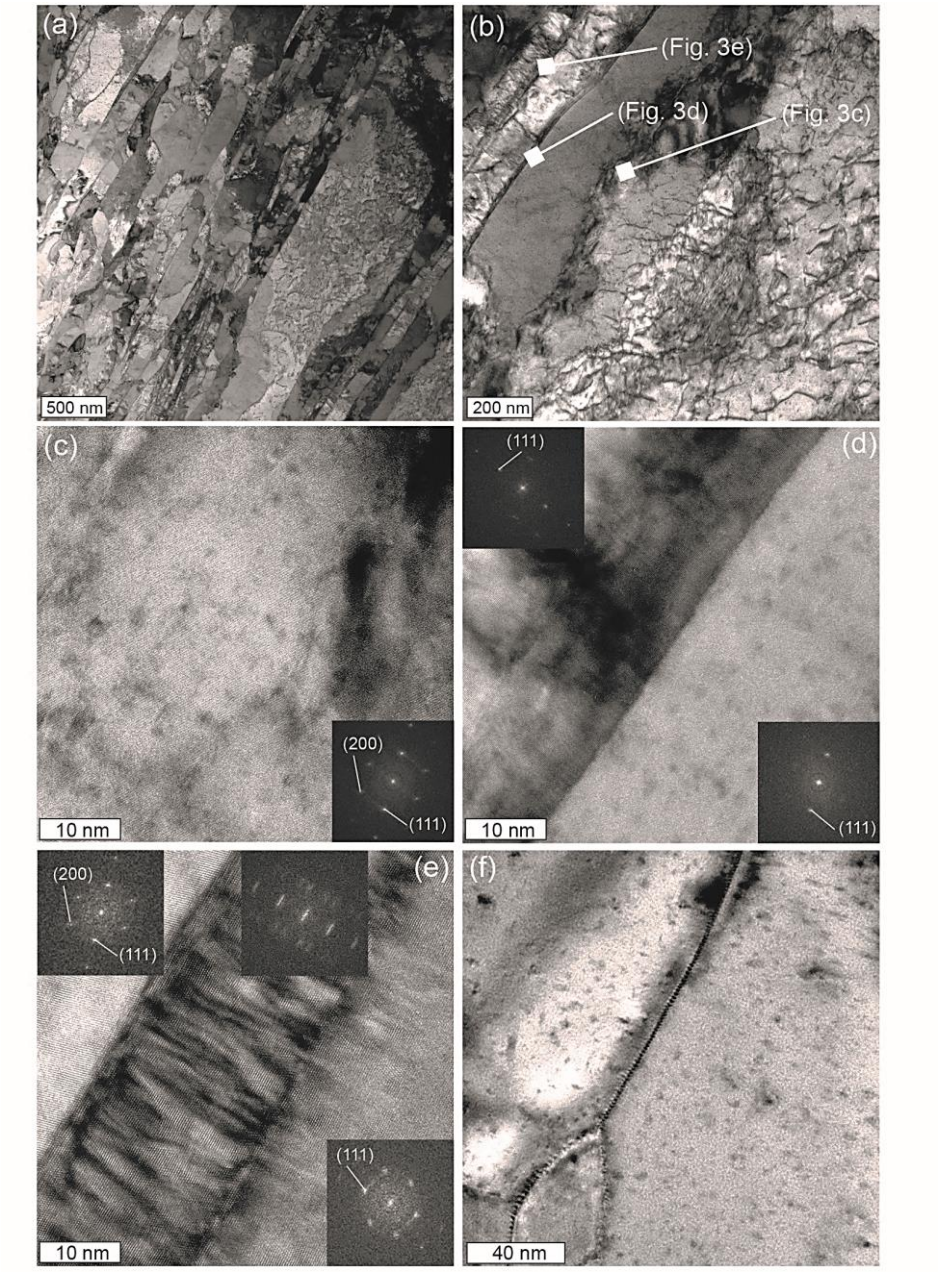

Figure 10. Low-magnification BFTEM image showing polycrystalline lamellar texture of the Ag-rich core of the Au nugget, No PGE particles within the sample area observed; (b) TEM of Grain boundaries between (Au,Ag)-lamellae. The white markers indicate the position of HR-TEM images. (c-e) HR-TEM images of "corrosion" like grain boundary; (c) Looks like replacement reaction boundary, however is a single crystal of gold with accumulated stain, diffraction pattern; (d) Fast Fourier Transform (FFT) analysis of the HR-TEM image revealed the presence of twinning; (e) Periodic array of edge dislocations associated with FFT of the HRTEM images. Note the multiple, diffused diffraction maxima (right corner) from a pile up of

dislocations which result in multiplication of the diffraction maxima; (f) BFTEM image of the dislocated grain boundaries between individual domains of gold.

The crystallisation can be seen to continue into the Ag depleted rim, however does not display the same clear structure as the core displays (Fig. 11a). This degradation of the crystal is seen across other portions of the sample. Misorientation of overlapping area shows the boundary between the changing crystal complexes (Fig. 11b).

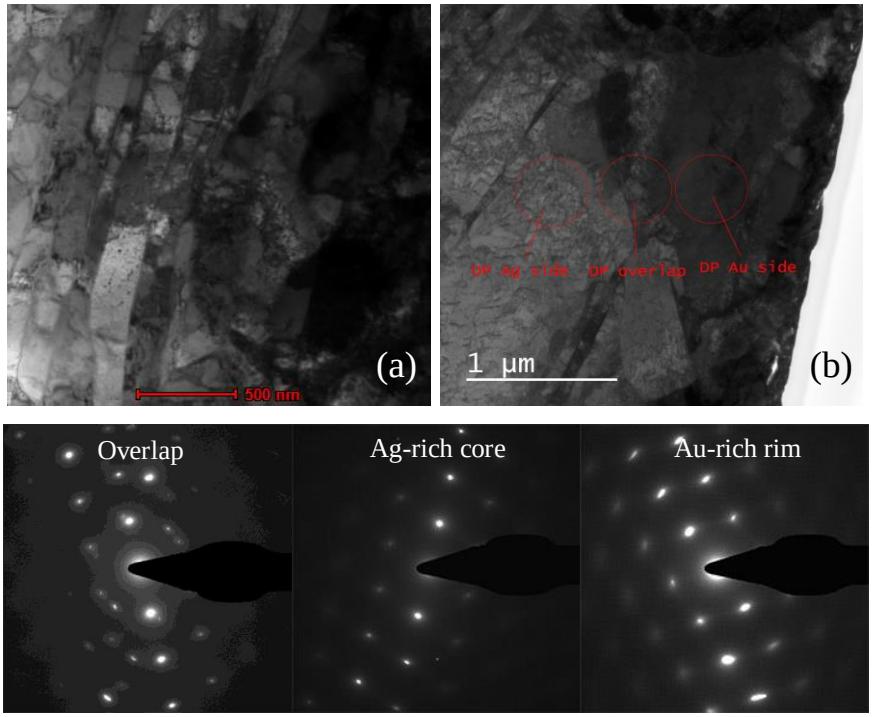

Figure 11. (a) Crystal growth in core; (b) lamellae gold crystallography in gold rich core High resolution TEM (HRTEM) with defined diffraction pattern SAED for the overlapping, Ag-rich core and Au-rich rim.

Chapter 5: Discussion

5.1 Structure of Au in Sample and Predictions

The rim observed on the samples were shown to have a PGE accumulation of between 10 to 20 µm. The PGEs accumulated in the rounded, poly crystalline nanoparticulate Au-rich rim. The rim exhibited greater porosity within this rim area. Despite porosity of the sample it was not observed to host accumulation of the PGE particles. It was only observed a homogeneous distribution of Ru, Rh and Pd in the gold matrix and with an apparent lack of PGEs nanoparticles in the pores (Fig. 9a).

Structurally the sample core displayed the identified lamellae in the Ag-rich core. The core contains minimum 19.5% of Ag (see Appendix 3) and was interpreted as an original texture of the sample prior to alterations. The nuggets studied all display an internal polycrystalline structure with coherent and incoherent twins that are characteristic of thermal annealing at elevated temperatures (Fig. 9a) (Hough et al. 2007).

Some studies observed elongated banding (lamellae) as a mylonitic style texture that formed due to electrorefining (Reith, Stewart, and Wakelin 2012), sequential dissolution and reprecipitation that lead to the rim forming on the sample (Groen, Craig, and Rimstidt 1990). In this sample the lamellae observed were much larger (tens to hundreds of microns) with Au-rich areas between the structures. For the work completed on the Ruby Creek samples there was no observed Au-rich areas with the lamellae nanometres large.

The nanoscale size of lamellae in Ag-rich core may be related to the content of Ag and other impurities, which stabilize the grain boundaries between the grains and prevent recrystallization. Some boundary areas distressing of gold from mechanically deformation can be observed (Fig. 10c).

This structural identity of the sample links the gold nugget to igneous host geology. The periodic array of edge dislocations of crystal intergrowth observed indicated growth under equilibrium conditions (Fig. 10e and 10f). The nanoscale size of lamellae in Ag-rich core may be related to the content of Ag

and other impurities, which stabilize the grain boundaries between the grains and prevent recrystallization. Alternatively, the rounded nanoparticulate Au-rich rim could experience recrystallization due to the lack of the impurities.

5.2 Thermodynamics of the Formation of Au Samples

The phase equilibrium for PGE containing samples is limited to thermodynamic binary phase diagrams of a pure binary system. Previous studies completed show the contrasting behaviour of PGEs (Ru, Rh and Pd) with Pd being partly miscible in both Au and Ag (Okamoto and Massalski 1984).

For a pure binary system containing Au-Pd alloys of equal composition form particles at temperatures of 850-870ºC. Formation is also possible under low temperature conditions of ~100ºC. Despite the opportunity of formation of particles of this alloy, no Au-Pd domains were observed within the samples. In a previous study supergene alteration of palladian gold (Au_7Pd) in laterites resulted in similar behaviour of Pd and Ag, which were depleted in the outer Au-rich layer (Cabral et al. 2002).

For the other detected PGEs, Rh and Ru, are completely immiscible in Au when in low temperature conditions of < 526ºC and < 626ºC, respectively. For Ru the maximum concentration that can be achieved in Au-Ru system for formation is 1.9 at. % at 1066ºC. The Ag-Ru system is moderately higher at 3.1 at. % at 920ºC (Okamoto and Massalski 1984).

The sample is not able to be classified into the binary systems for formation temperatures due to the impurities present. The presence of the investigated PGEs in solid solution (Figs. 4 and 5) is likely due to their relatively low concentrations and/or association with other trace elements such as As, Se and S, which may help to dissolve PGEs in the gold structure. It is expected that gold particles enriched with Ag may host more Pd in solid solution as Pd is completely miscible in Ag.

The distribution seen of the PGEs suggests that during alteration of gold particles under supergene conditions, PGEs are either:

(i) delivered to the surface of the Au nugget by altering solutions as colloids; including processes of dissolution and reprecipitation; or are

(ii) subjected to the enrichment process due to a selective dissolution of Ag.

Homogeneous distribution of Ru, Rh and Pd in the gold matrix and lack of PGEs nanoparticles in the pores advocates for the second scenario (Fig. 9).

Chapter 6: Conclusion

The irrefutable evidence obtained from this study is that the PGEs are in solid solution in crystal structure in this sample. Exsolution does not occur at the nanoscale. It can also be said that during the process of alteration, the PGE accumulate in the Ag removed area.

Understanding the minor and trace element geochemistry of gold nuggets is of key importance when attempting to elucidate the conditions of gold deposit formation and establishing new areas for Au exploration. Geologically "instantaneous" formation of porphyry and epithermal deposits that are subjected to sedimentary destruction creates a variety of sources that makes gold nugget origins almost impossible to pin point. The phase attributes and crystallography help to define the unique nature of the gold particle at both a macro and nanoscale particle scale. Gold's association with precious and base metals need more research to understand why they associate and the complex structures at an atomic scale.

6.1 Future work

The interest in this project will extend into Nano-SIMS academic activity to have a closer look at the isotopic complexity and to look at the distribution of isotopes of PGEs in gold sample. Re and PGE (particularly osmium) are the key elements that will be focussed on. The will also be a focus on the isotopes of all the PGEs that can be seen with a lower detection limit

Looking for exsolution at absolute nanoscales and to see if the isotopes of the PGEs fractionate in the gold formation are also main features of the future work in this area of mineralogy.

References

Armstrong, JT. 1988. "Quantitative analysis of silicate and oxide minerals: comparison of Monte Carlo, ZAF and phi-rho-z procedures." *Microbeam analysis* 23:239-246.

Bakos, F. M Chovan, P Bačo, B Bahna, Š Ferenc, P Hvožďara, S Jeleň, M Kamhalová, R Kaňa, and J Knésl. 2004. "Gold in Slovakia." *Slovenský Skauting, Bratislava*:1-298.

Boyles, RW. 1979. "The geochemistry of gold and its deposits." *Geological Survey of Canada Bulletin* 280:1-584.

Butt, Charles R. M., and Robert M. Hough. 2009. "Why Gold is Valuable." *Elements* 5 (5):277.

Cabral, Alexandre Raphael, Bernd Lehmann, Rogerio Kwitko-Ribeiro, and Carlos Henrique Cravo Costa. 2002. "Palladium and Platinum Minerals from the Serra Pelada Au–Pd–Pt Deposit, Carajás Mineral Province, Northern Brazil." *The Canadian Mineralogist* 40 (5):1451.

Canet, Carles, Pura Alfonso, Joan-Carles Melgarejo, and Susana Jorge. 2003. "Pge-Bearing Minerals in Silurian Sedex Deposits in the Poblet Area, Southwestern Catalonia, Spain." *The Canadian Mineralogist* 41 (3):581.

Chapman, RJ, RC Leake, and NR Moles. 2000. "The use of microchemical analysis of alluvial gold grains in mineral exploration: experiences in Britain and Ireland." *Journal of Geochemical Exploration* 71 (3):241-268.

Cobley, Claire M., and Younan Xia. 2009. "Gold and Nanotechnology." *Elements* 5 (5):309.

Donovan, John J, Jared W Singer, and John T Armstrong. 2016. "A new EPMA method for fast trace element analysis in simple matrices." *American Mineralogist* 101 (8):1839-1853.

Donovan, John J, Donald A Snyder, and Mark L Rivers. 1992. "An improved interference correction for trace element analysis." Proceedings of the Annual Meeting-Electron Microscopy Society of America.

Donovan, John J, and Tracy N Tingle. 1996. "An improved mean atomic number background correction for quantitative microanalysis." *Microscopy and Microanalysis* 2 (1):1-7.

Dowdell, Ralph Lewis, Henry Samuel Jerabek, Arthur C Forsyth, and Carrie H Green. 1943. *General metallography*: J. Wiley & sons, inc.

Eby, G Nelson. 2016. *Principles of environmental geochemistry*: Waveland Press.

Eyles, N. 1990. "Post-depositional nugget accretion in Cenozoic placer gold deposits, Cariboo mining district, British Columbia (93 A, B, G, H)." *BC Ministry of Energy, Mines and Petroleum Resources*:147-169.

Eyles, Nicholas, and Stephen P Kocsis. 1988. "Sedimentological Controls on Gold Distribution in Pleistocene Placer Deposits of the Cariboo Mining District, British Columb: La."

REFERENCES

Fairbrother, L, J Brugger, J Shapter, JS Laird, G Southam, and F Reith. 2012. "Supergene gold transformation: Biogenic secondary and nano-particulate gold from arid Australia." *Chemical Geology* 320:17-31.

Goldfarb, Richard, D. Groves, and Stephen Gardoll. 2001. *Orogenic gold and geologic time: A global synthesis*. Vol. 18.

Groen, John C, James R Craig, and J Donald Rimstidt. 1990. "Gold-rich rim formation on electrum grains in placers." *The Canadian Mineralogist* 28 (2):207-228.

Guha, A. 1985. "Metals handbook, vol. 8." *Ohio: ASM International, Materials Park*:133.

Hora, ZD, E Pivec, and A Langrova. 2011. "Irarsite (IrAsS), Osarsite (OsAsS) and Gold from Placer Black Sands, Ruby Creek and Wright Creek, Atlin, British Columbia." *Geological Fieldwork*:2012-1.

Hough, R. M., C. R. M. Butt, S. M. Reddy, and M. Verrall. 2007. "Gold nuggets: supergene or hypogene?" *Australian Journal of Earth Sciences* 54 (7):959-964. doi: 10.1080/08120090701488289.

Hough, Robert M., Charles R. M. Butt, and Jörg Fischer-Bühner. 2009. "The Crystallography, Metallography and Composition of Gold." *Elements* 5 (5):297.

Knight, JB, SR Morison, and JK Mortensen. 1999. "The relationship between placer gold particle shape, rimming, and distance of fluvial transport as exemplified by gold from the Klondike District, Yukon Territory, Canada." *Economic Geology* 94 (5):635-648.

Knight, John, and Craig H. B. Leitch. 2001. "Phase Relations in the System Au–Cu–Ag at Low Temperatures, based on Natural Assemblages." *The Canadian Mineralogist* 39 (3):889.

Levson, V, DE Kerr, C Lowe, and H Blyth. 2003. "Quaternary geology of the Atlin area, British Columbia." *Geological Survey of Canada, Open File* 1562 (1).

Mihalynuk, Mitchell G, Alexandre Zagorevski, Fionnuala AM Devine, and Elaine Humphrey. 2017. "A new lode gold discovery at Otter Creek: Another source for the Atlin placers." *Geological Survey Paper* 1:179-193.

Murdoch, Joseph, and Robert Wallace Webb. 1966. *Minerals of California: Centennial Volume (1866-1966)*. Vol. 189: California Division of Mines and Geology.

Murzin, Vv, Vi Kudryavtsev, Ro Berzon, Sg Sustavov, and Aa Malyugin. 1983. "New data on the instability of natural solid solutions of the gold–silver–copper system at temperatures below 350 C." Dokl. Acad. Sci. USSR, Earth Sci. Sect.

Okamoto, H., and T. B. Massalski. 1984. "The Au-Os (Gold-Osmium) System." *Bulletin of Alloy Phase Diagrams* 5 (4):382-382. doi: 10.1007/bf02872957.

Palacios, Carlos, Gérard Hérail, Brian Townley, Víctor Maksaev, Fabián Sepúlveda, Philippe de Parseval, Pablo Rivas, Alfredo Lahsen, and Miguel Angel Parada. 2001. "The Composition of Gold in the Cerro Casale Gold-

Rich Porphyry Deposit, Maricunga Belt, Northern Chile." *The Canadian Mineralogist* 39 (3):907.

Phillips, G. Neil, and Roger Powell. 2009. "Formation of gold deposits: Review and evaluation of the continuum model." *Earth-Science Reviews* 94 (1):1-21. doi: https://doi.org/10.1016/j.earscirev.2009.02.002.

Rauch, Sebastien, and Gregory M. Morrison. 2008. "Environmental Relevance of the Platinum-Group Elements." *Elements* 4 (4):259.

Reith, Frank, Barbara Etschmann, Cornelia Grosse, Hugo Moors, Mohammed A. Benotmane, Pieter Monsieurs, Gregor Grass, Christian Doonan, Stefan Vogt, Barry Lai, Gema Martinez-Criado, Graham N. George, Dietrich H. Nies, Max Mergeay, Allan Pring, Gordon Southam, and Joël Brugger. 2009. "Mechanisms of gold biomineralization in the bacterium Cupriavidus metallidurans." *Proceedings of the National Academy of Sciences* 106 (42):17757-17762.

Reith, Frank, Stephen L Rogers, DC McPhail, and Daryl Webb. 2006. "Biomineralization of gold: biofilms on bacterioform gold." *science* 313 (5784):233-236.

Reith, Frank, Lachlan Stewart, and Steven A Wakelin. 2012. "Supergene gold transformation: Secondary and nano-particulate gold from southern New Zealand." *Chemical Geology* 320:32-45.

Shcheka, Galina G., Bernd Lehmann, Eike Gierth, Karsten Gömann, and Alex Wallianos. 2004. "Macrocrystals of Pt–Fe Alloy from the Kondyor Pge Placer Deposit, Khabarovskiy Kray, Russia: Trace-Element Content, Mineral Inclusions and Reaction Assemblages." *The Canadian Mineralogist* 42 (2):601.

Sillitoe, Richard H, and Jeffrey W Hedenquist. 2003. "Linkages between volcanotectonic settings, ore-fluid compositions, and epithermal precious metal deposits." *Special Publication-Society of Economic Geologists* 10:315-343.

Simmons, Stuart F, Noel C White, and David A John. 2005. "Geological characteristics of epithermal precious and base metal deposits." *Economic Geology 100th anniversary volume* 29:485-522.

Smith, Dorian GW, and Ernest H Nickel. 2007. "A system of codification for unnamed minerals: Report of the Subcommittee for Unnamed Minerals of the IMA Commission on New Minerals, Nomenclature and Classification." *The Canadian Mineralogist* 45 (4):983-990.

Southam, Gordon, Maggy F. Lengke, Lintern Fairbrother, and Frank Reith. 2009. "The Biogeochemistry of Gold." *Elements* 5 (5):303.

Sun, WeiDong, MingXing Ling, XiaoYong Yang, WeiMing Fan, Xing Ding, and HuaYing Liang. 2010. "Ridge subduction and porphyry copper-gold mineralization: An overview." *Science China Earth Sciences* 53 (4):475-484. doi: 10.1007/s11430-010-0024-0.

REFERENCES

Tosdal, Richard M., John H. Dilles, and David R. Cooke. 2009. "From Source to Sinks in Auriferous Magmatic-Hydrothermal Porphyry and Epithermal Deposits." *Elements* 5 (5):289.

Townley, Brian K, Gerard Hérail, Victor Maksaev, Carlos Palacios, Philippe de Parseval, Fabían Sepulveda, Rodrigo Orellana, Pablo Rivas, and Cesar Ulloa. 2003. "Gold grain morphology and composition as an exploration tool: application to gold exploration in covered areas." *Geochemistry: Exploration, Environment, Analysis* 3 (1):29-38.

Vikentyev, Ilya V., Marina A. Yudovskaya, Andrey V. Mokhov, Alexey L. Kerzin, and Anatoliy I. Tsepin. 2004. "Gold and Pge in Massive Sulfide Ore of the Uzelginsk Deposit, Southern Urals, Russia." *The Canadian Mineralogist* 42 (2):651.

Walshe, John L., and James S. Cleverley. 2009. "Gold Deposits: Where, When and Why." *Elements* 5 (5):288.

White, J. L., R. L. Orr, and R. Hultgren. 1957. "The thermodynamic properties of silver-gold alloys." *Acta Metallurgica* 5 (12):747-760. doi: http://dx.doi.org/10.1016/0001-6160(57)90078-0.

White, Noel C, and Jeffrey W Hedenquist. 1995. "Epithermal gold deposits: styles, characteristics and exploration." *SEG newsletter* 23 (1):9-13.

Williams-Jones, Anthony E, and Christoph A Heinrich. 2005. "100th Anniversary special paper: vapor transport of metals and the formation of magmatic-hydrothermal ore deposits." *Economic Geology* 100 (7):1287-1312.

Williams-Jones, Anthony E., Robert J. Bowell, and Artashes A. Migdisov. 2009. "Gold in Solution." *Elements* 5 (5):281.

Appendix 1: Paragenisis and surrounding mineralogy graphs

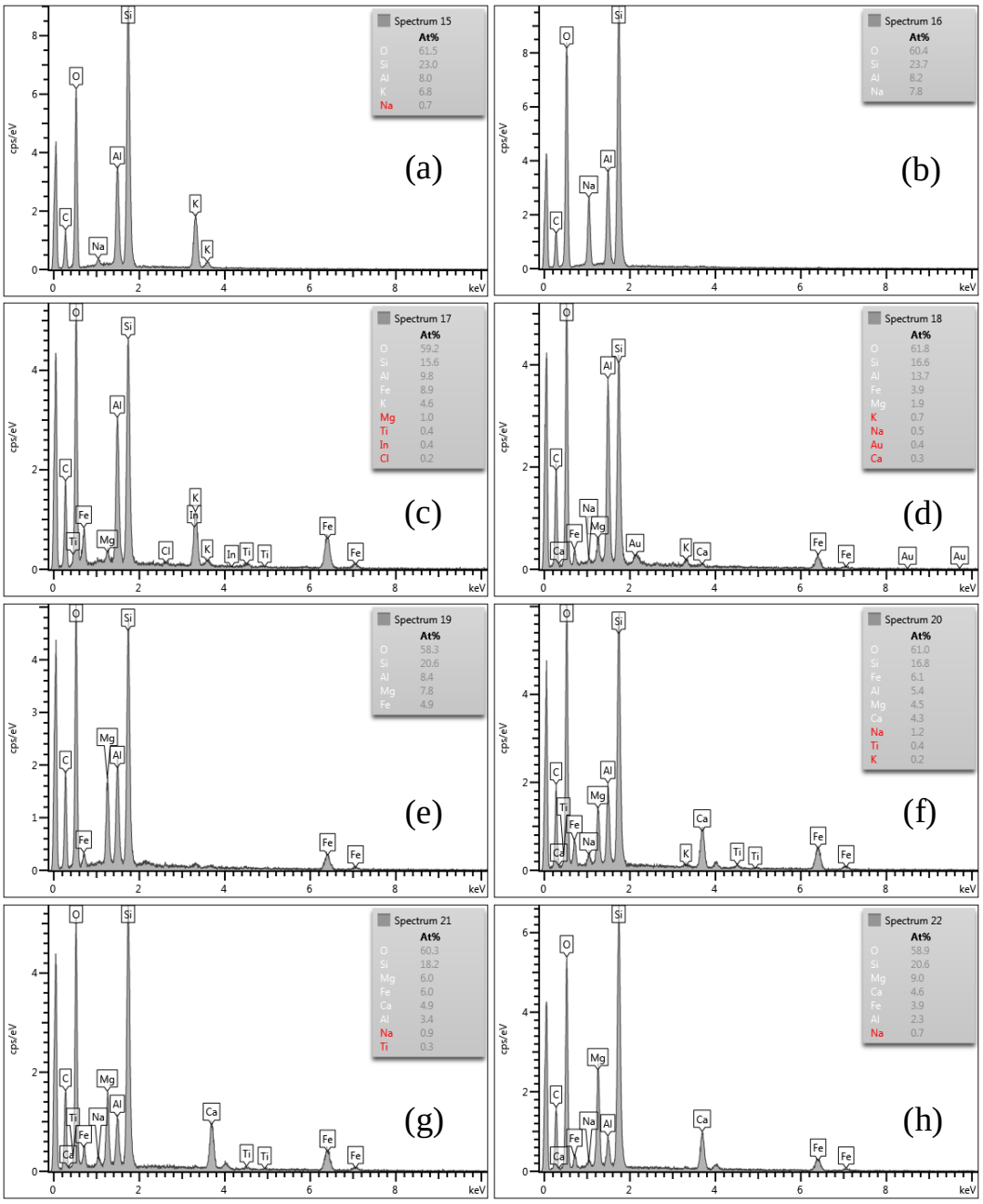

Figure 12. a); Mineralogy Composition (At%) Spectrum 15, Orthoclase ($KAlSi_3O_8$); (b) Mineralogy Composition (At%) Spectrum 16, Plagioclase (Albite) (NaAlSi3O8); (c) Mineralogy Composition (At%) Spectrum 17, Biotite (K(Mg,Fe)3(AlSi3O10)(F,OH)2); (d) Mineralogy Composition (At%) Spectrum 18, Chlorite ($(Mg,Fe)_3(Si,Al)_4O_{10}(OH)_2 \cdot (Mg,Fe)_3(OH)_6$); (e) Mineralogy Composition (At%) Spectrum 19 Possible Garnet (X3Y2(SiO4)3) or Chlorites; (f) Mineralogy Composition (At%) Spectrum 20, Hornblende, ($(Ca,Na)_{2-3}(Mg,Fe,Al)_5(Si,Al)_8O_{22}(OH,F)_2$); (g) Mineralogy Composition (At%) Spectrum 21, Quartz, (SiO_2); (h) Mineralogy Composition (At%) Spectrum 22, Hornblende.

Appendix 2: FIB Sample Preparation

The FIB cutting was done to have a sample thin enough for TEM. The selected area was cut across where the Ag depleted rim had a clear boundary to the core. The area was less porous and was ideal for the section cutting for a clear representation of both areas.

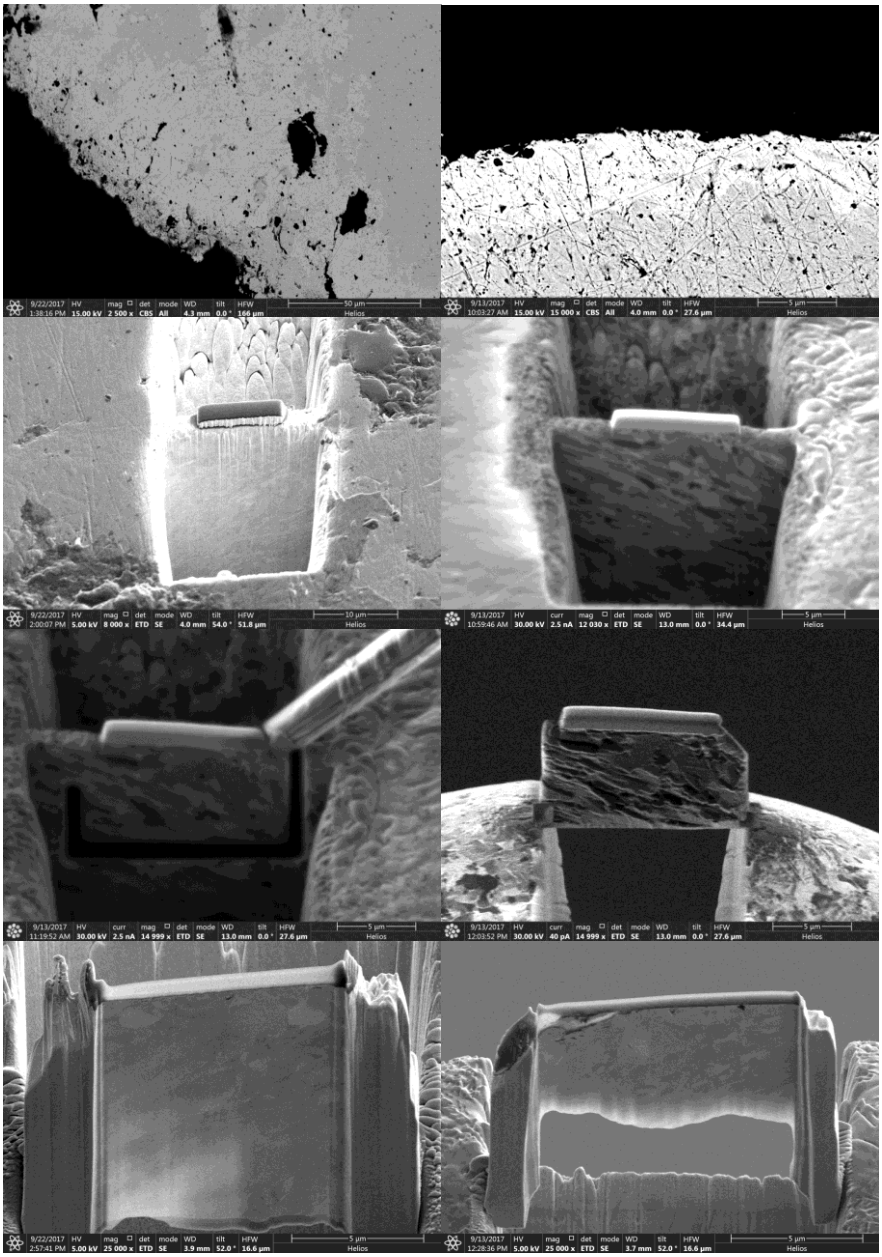

Figure 13. (a) BSE Image, Au/Ag boundary; (b)BSE Image, Au/Ag Boundary Sample Zone; (c) SE Image Carbon top, initial trenching, (d) SE Image Finished trenching (e) SE Image, U cut and welded on needle; (f) SE Image, , Welded onto pin; (g) SE Image,, Prior to Thinning; (h) SE Image, Final Thin Section for TEM.

Appendix 3: EMPA Microprobe Analysis Table:

The microprobe was completed at the CMCA facilities to establish the mineralogical content of the Au Sample.

Table 2: EMPA Microprobe Analysis

Det	0.022	0	0.014	0.011	0	0.045	0.074	0.013	0.040	0.010	0.010	0.081	0	0.009	0.077	0.111	0.089	0.014	0.054	0.034	0.037	0.038	0.043	0.024	0.015	0.006				
	S	As	Sb	Fe	Se	Au	Te	Cu	Pb	Ni	Co	Ag	Bi	Si	Pd	Ru	Rh	Cr	Hg	Re	Os	Ir	Pt	V	Mn	Ti	correct	other	PGEs	S +
T1	0.07	0.49	0.06		0.51	79.37			0.11			21.66	0.13	0.12		0.27			0.17							0.02	102.97	23.61	0.27	1.06
T1	0.02	0.08			0.09	80.53			0.06			21.11		0.04					0.12								102.05	21.52	0.00	0.19
T1	0.07	0.15			0.13	80.33						20.92		0.13					0.16								101.90	21.57	0.00	0.36
T1	0.03	0.10			0.12	80.07			0.05			21.02		0.04					0.06								101.49	21.43	0.00	0.25
T1		0.12	0.02		0.10	80.28			0.06			21.56							0.09								102.21	21.94	0.00	0.22
T1	0.05	0.26			0.29	79.87			0.04			22.08		0.08		0.13										0.01	102.81	22.93	0.13	0.60
T1		0.11	0.02		0.13	80.39			0.05	0.01		21.56							0.09								102.37	21.99	0.00	0.24
T1	0.03	0.14			0.15	80.96			0.06			20.70		0.03													102.05	21.10	0.00	0.31
T1	0.06	0.08			0.07	80.50						21.37		0.01					0.14								102.22	21.72	0.00	0.21
T1	0.02	0.10			0.08	80.55						20.98		0.04					0.04								101.83	21.27	0.00	0.21
T1		0.02				80.30						21.24		0.05					0.19								101.80	21.51	0.00	0.02
T1	0.02	0.12			0.09	80.11			0.05			21.55		0.02					0.08								102.05	21.94	0.00	0.23
T1	0.04	0.10			0.10	80.04						22.12		0.03		0.15	0.14		0.11								102.83	22.79	0.29	0.25
T1		0.00				79.92						21.44							0.08								101.45	21.53	0.00	0.00
T1		0.08			0.08	80.14			0.07			21.32							0.07								101.75	21.61	0.00	0.16
T1	0.04	0.12	0.02		0.11	79.99			0.06			21.64		0.07		0.26	0.12										102.42	22.43	0.37	0.26
T1		0.23	0.04		0.19	79.91			0.13			21.45	0.10	0.05				0.02	0.11							0.01	102.24	22.33	0.00	0.41
T1	0.04	0.14			0.11	79.43			0.06			21.13		0.03										0.03			100.96	21.53	0.00	0.29
T1	0.05	0.11			0.06	79.83						21.21							0.14								101.40	21.57	0.00	0.22
T1	0.12	0.23			0.25	79.98						21.77		0.05	0.09	0.23	0.11		0.17								103.00	23.02	0.44	0.60
T1	0.03	0.21	0.03		0.23	80.06			0.09		0.01	21.81		0.05	0.11	0.13			0.12							0.01	102.87	22.82	0.24	0.46
T1	0.03	0.12			0.13	80.38						21.90		0.01					0.09								102.66	22.28	0.00	0.28
T1	0.11	0.05			0.12	80.09						21.49		0.04					0.22								102.13	22.04	0.00	0.28
T1		0.13			0.07	80.72						20.39		0.01					0.09								101.41	20.69	0.00	0.20
T1		0.00				80.17						20.79							0.07								101.03	20.86	0.00	0.00
T1		0.00	0.02			80.75						21.44							0.11								102.32	21.57	0.00	0.00
T1	0.08	0.15			0.17	80.27						22.16		0.04					0.12								102.99	22.72	0.00	0.40
T1	0.05	0.25	0.04		0.24	79.98			0.05			22.21		0.04		0.19			0.15							0.01	103.20	23.22	0.19	0.53
T1		0.15	0.02		0.14	81.08			0.06			20.76		0.02					0.11								102.33	21.25	0.00	0.29
T1	0.03	0.39	0.08	0.04	0.38	97.79			0.10		0.01	2.62	0.20	0.20		0.11			0.07							0.02	102.04	4.25	0.11	0.80
T1	0.13	0.00		0.01		96.86						3.11		0.08					0.35								100.53	3.67	0.00	0.13
T1	0.08	0.04				97.83						2.31		0.04	0.13	0.31	0.28		0.06								101.07	3.24	0.72	0.12
T1	0.05	0.09	0.02		0.12	95.95			0.04			4.16	0.08	0.08													100.59	4.64	0.00	0.26
T1	0.09	0.17	0.03	0.03	0.16	97.73						1.10	0.03	0.11	0.34	0.61	0.49										100.88	3.15	1.44	0.42
T1	0.05	0.17	0.03		0.16	98.08			0.04	0.01		3.05	0.12	0.15				0.02	0.14							0.01	102.03	3.95	0.00	0.39
T1	0.11	0.20	0.02		0.23	98.61						2.05	0.06	0.09	0.25	0.31	0.24		0.13							0.01	102.30	3.70	0.80	0.54
T1			0.04			97.47			0.13			0.90	0.18					0.02	0.06							0.01	98.82	1.35	0.00	0.00
T1	0.14	0.31		0.02	0.35	98.81						2.08		0.17	0.47	0.78	0.56		0.07							0.01	103.75	4.94	1.81	0.79
T1	0.06	0.23	0.01		0.21	98.91						2.17	0.03	0.15	0.13	0.42	0.18		0.08				0.04			0.01	102.64	3.73	0.78	0.50
T1	0.11	0.45	0.06	0.20	0.50	92.24			0.18			2.74	0.21	0.79					0.11							0.06	97.64	5.41	0.00	1.05
T1	0.12	0.28		0.58	0.28	85.05			0.05			5.48		0.82	0.25	0.74	0.46										94.11	9.06	1.45	0.68
T1	0.14			0.74	0.07	80.40			0.09			9.84	0.14	1.24					0.25								92.92	12.51	0.00	0.21
T1	0.18	0.17	0.03		0.13	92.92			0.05			10.09	0.07	0.14	0.08	0.30	0.21		0.29								104.64	11.73	0.59	0.47
T1	0.35	0.33	0.05	0.04	0.30	93.10			0.11			8.49	0.07	0.28	0.11	0.14			0.63							0.02	104.02	10.92	0.24	0.99
T1	0.30	0.30	0.03	0.06	0.35	93.62			0.05			7.88	0.06	0.41	0.30	0.46	0.38		0.35							0.01	104.54	10.92	1.13	0.95
T1	0.13	0.73	0.08	0.01	0.74	97.09			0.19			1.81	0.26	0.17	0.62	1.13	0.73									0.03	103.73	6.63	2.47	1.60
T1	0.24	0.41	0.04		0.44	97.19			0.02			2.58	0.04	0.16	0.60	1.06	0.68		0.11							0.01	103.60	6.41	2.35	1.10

APPENDIX

T1	0.18	0.12	0.02	0.24	0.13	96.01	0.09		0.04			1.89	0.09	0.19	0.21	0.22	0.34									99.77	3.75	0.77	0.42
T1	0.23	0.38		0.76	0.45	93.25						2.00		0.42	0.45	0.81	0.56		0.14						0.05		99.50	6.25	1.82	1.06
T1	0.24	0.02		0.20	0.01	87.03						4.11		0.22	0.19		0.27										92.29	5.26	0.45	0.27
T2		0.09			0.07	79.93			0.05			21.14															101.27	21.34	0.00	0.15
T2	0.10	0.19	0.03		0.27	79.85			0.04			21.92		0.04	0.10	0.32	0.11		0.09							0.01	103.06	23.21	0.52	0.56
T2	0.17	0.00				80.01						20.73		0.13					0.34								101.37	21.36	0.00	0.17
T2		0.02				80.12						19.98		0.02													100.14	20.02	0.00	0.02
T2	0.04	0.09	0.02		0.12	80.02			0.05			21.59														0.01	101.95	21.93	0.00	0.26
T2	0.12	0.22			0.18	80.09						20.39		0.12		0.12			0.13								101.35	21.26	0.12	0.51
T2	0.02	0.04			0.04	80.93						20.56		0.10					0.14								101.83	20.90	0.00	0.11
T2		0.12			0.12	79.96						21.71		0.03												0.01	101.95	21.99	0.00	0.24
T2	0.06					80.06						22.05				0.23	0.13		0.07								102.62	22.56	0.37	0.06
T2					0.01	81.01						20.45		0.13					0.08								101.70	20.68	0.00	0.01
T2	0.11	0.11	0.02		0.19	80.12					0.01	21.47		0.06	0.13	0.25	0.11		0.14								102.71	22.59	0.49	0.41
T2	0.06	0.10			0.11	80.28					0.01	20.90		0.10					0.15								101.71	21.43	0.00	0.27
T2	0.05				0.01	82.60						17.63		0.08					0.02								100.38	17.79	0.00	0.06
T2						93.79						5.49		0.03													99.30	5.51	0.00	0.00
T2	0.03		0.03			98.12			0.05			2.75	0.06	0.10					0.15					0.03		0.01	101.33	3.22	0.00	0.03
T2	0.03	0.19	0.05		0.17	98.71			0.08	0.01	0.01	1.27	0.18	0.06		0.19			0.08					0.03		0.01	101.07	2.36	0.19	0.40
T2	0.10					101.4						2.09		0.05					0.56	0.08		0.13	0.15		0.02		104.57	3.18	0.35	0.10
T2		0.05	0.02			97.31						4.55		0.10					0.16							0.01	102.21	4.89	0.00	0.05
T2						93.71						2.87							0.08								96.66	2.95	0.00	0.00
T2	0.17					93.87						6.14		0.05					0.30								100.53	6.65	0.00	0.17
T2	0.18	0.29	0.01		0.40	96.33						5.62		0.16	0.45	0.44	0.23		0.17				0.05			0.01	104.33	8.00	1.16	0.87
T2	0.08	0.06			0.13	97.69						2.05		0.12	0.14	0.20											100.48	2.78	0.34	0.28
T2	0.17	0.29		0.49	0.22	92.93						4.44		0.28	0.29	0.60	0.23		0.09								100.04	7.11	1.12	0.69
T2	0.17	0.29	0.05	0.26	0.36	92.74			0.09			8.06	0.14	0.46	0.15	0.42	0.23		0.20							0.02	103.64	10.89	0.80	0.83
T2	0.14	0.07			0.02	98.37						1.33		0.04	0.56	0.99	0.69										102.21	3.84	2.24	0.22
T2	0.10	0.21			0.33	98.62						1.28	0.08	0.10	0.35	0.51	0.45		0.06								102.08	3.46	1.31	0.64
T2	0.39	0.59	0.25	0.31	0.64	126.8	0.23	0.01	0.30	0.12	0.10	3.44	0.59	0.46	0.72	1.33	1.08	0.08	1.32	0.55	0.56	0.67	0.83	0.09	0.10	0.15	141.78	14.91	5.74	1.62
T2	0.17	0.31			0.32	97.42						2.18		0.13	0.67	1.24	0.87										103.31	5.90	2.78	0.81
T2	0.07			0.81		89.45						1.39		0.98													92.70	3.25	0.00	0.07
T2	0.21	0.04		0.24	0.05	91.15						3.29		0.24	0.23		0.24										95.69	4.53	0.47	0.30
T3				0.14		95.05						0.56		0.10											0.02		95.87	0.83	0.00	0.00
T3						80.09						20.70							0.06								100.85	20.76	0.00	0.00
T3	0.08					80.41						21.18							0.17								101.84	21.43	0.00	0.08
T3	0.05	0.21		0.01	0.22	80.41	0.08				0.01	21.29		0.03					0.15							0.01	102.47	22.06	0.00	0.49
T3	0.02					80.47						20.77		0.07					0.06								101.40	20.93	0.00	0.02
T3	0.07	0.03			0.04	80.34						21.75				0.13			0.14								102.50	22.15	0.13	0.14
T3	0.03	0.03			0.02	80.45			0.04			21.46							0.11								102.15	21.70	0.00	0.09
T3	0.14	0.04			0.07	80.37						21.81					0.12		0.14								102.69	22.31	0.12	0.24
T3						80.60						19.60							0.11								100.31	19.71	0.00	0.00
T3	0.05	0.08			0.11	80.86			0.07			21.09		0.02					0.12								102.39	21.53	0.00	0.24
T3		0.02			0.02	80.81						21.05							0.10								102.00	21.19	0.00	0.04
T3	0.07	0.04				79.68						21.16		0.01					0.06								101.01	21.34	0.00	0.11
T3						79.86					0.01	21.62															101.49	21.63	0.00	0.00
T3	0.04	0.35	0.07		0.37	80.07	0.13		0.16		0.01	21.56	0.16	0.06					0.14							0.03	103.15	23.07	0.00	0.75
T3	0.09	0.11	0.01		0.12	79.62			0.05			22.21		0.05		0.17			0.11								102.57	22.94	0.17	0.33
T3	0.05	0.11	0.02		0.10	80.64			0.06			21.52		0.01					0.07								102.58	21.94	0.00	0.26
T3	0.13	1.33	0.20		1.44	77.25			0.38			21.70	0.54	0.30	0.22	0.52	0.17		0.10							0.07	104.35	27.10	0.91	2.90
T3	0.04	0.11			0.06	80.60			0.06			21.37		0.02					0.08								102.34	21.74	0.00	0.21
T3	0.02	0.05			0.06	80.68			0.04			21.08							0.07							0.01	102.01	21.33	0.00	0.13
T3						80.74						19.48		0.04					0.11								100.37	19.63	0.00	0.00
T3	0.08				0.02	79.77						21.34		0.01	0.21	0.63	0.50										102.57	22.80	1.34	0.11
T3	0.04	0.25	0.02		0.28	79.92			0.08			21.47	0.06	0.09	0.08	0.15		0.01								0.02	102.47	22.55	0.23	0.57

APPENDIX

T3	0.04	0.14			0.17	80.49			0.06			21.38		0.02					0.07							0.01	102.38	21.89	0.00	0.35
T3	0.07				0.05	80.46						21.34							0.10								102.02	21.56	0.00	0.12
T3	0.05	0.07			0.04	80.61						20.08															100.86	20.24	0.00	0.16
T3	0.08	0.03			0.05	80.44						20.72							0.10								101.41	20.97	0.00	0.16
T3	0.03	0.10			0.05	80.30						22.12											0.04				102.65	22.35	0.04	0.19
T3	0.02	0.17	0.02		0.14	80.23						21.33		0.01		0.18			0.09								102.18	21.95	0.18	0.33
T3		0.05			0.03	80.45						20.94							0.08								101.55	21.10	0.00	0.08
T3	0.06	0.09			0.10	80.80						21.22		0.04					0.09								102.40	21.60	0.00	0.25
T3	0.04	0.06	0.02		0.08	80.80						20.98		0.03					0.09					0.03		0.01	102.13	21.33	0.00	0.17
T3	0.08	0.22	0.01		0.24	80.14					0.02	22.00		0.03	0.11	0.29	0.10		0.08							0.01	103.32	23.18	0.49	0.54
T3	0.09	0.04			0.02	79.87						20.10		0.03					0.20								100.37	20.49	0.00	0.16
T3			0.01			81.25			0.08			20.32		0.02					0.10								101.78	20.53	0.00	0.00
T3			0.03			79.99			0.09			20.10	0.02						0.13								100.36	20.37	0.00	0.00
T3	0.15	0.13			0.16	79.92						21.41		0.05					0.21								102.03	22.11	0.00	0.44
T3			0.02			79.72			0.07	0.01		20.26							0.08								100.16	20.44	0.00	0.00
T3	0.10					79.75						20.31		0.04					0.15								100.36	20.61	0.00	0.10
T3	0.05	0.02			0.03	80.81					0.01	21.16		0.03					0.10								102.21	21.40	0.00	0.10
T3	0.10	0.27	0.02		0.31	80.09			0.07			22.04		0.04	0.18	0.26			0.10								103.48	23.39	0.44	0.68
T3	0.10	0.11	0.02		0.14	79.76			0.06			21.47		0.09					0.13								101.88	22.12	0.00	0.35
T3	0.09					79.89						20.56							0.14								100.69	20.79	0.00	0.09
T3	0.07					80.39						20.94							0.06								101.46	21.07	0.00	0.07
T3		0.06			0.07	80.55			0.07			21.33		0.01					0.06							0.01	102.15	21.60	0.00	0.13
T3						80.19			0.06			20.75							0.07								101.07	20.88	0.00	0.00
T3		0.19	0.04		0.18	80.24			0.07			21.87	0.05	0.03					0.11							0.01	102.78	22.53	0.00	0.36
T3	0.06	0.22	0.02		0.24	80.58			0.06			21.66		0.10		0.27			0.07							0.01	103.27	22.69	0.27	0.51
T3	0.06	0.07			0.03	80.76					0.01	21.26		0.05					0.07								102.30	21.55	0.00	0.16
T3	0.09	0.16			0.15	80.60			0.04			21.77		0.02	0.08	0.21			0.07								103.19	22.59	0.29	0.39
T3		0.12			0.07	80.76						21.88							0.13								102.96	22.20	0.00	0.19
T3	0.17	0.10			0.08	80.90						22.17		0.02	0.09	0.31			0.16				0.04				104.04	23.14	0.45	0.35
T3	0.03	0.06			0.12	80.84						21.48		0.01					0.09							0.01	102.64	21.80	0.00	0.22
T3	0.08	0.26	0.03		0.27	80.60			0.11			22.19		0.07					0.13							0.01	103.76	23.17	0.00	0.62
T3	0.06	0.57	0.10		0.57	78.85			0.18			21.67	0.20	0.12		0.20			0.11							0.04	102.65	23.81	0.20	1.19
T3	0.12	0.18			0.13	80.52			0.04			21.29		0.06					0.13								102.48	21.95	0.00	0.43
T3	0.06	0.09			0.01	80.58						21.29							0.07						0.02		102.12	21.54	0.00	0.16
T3		0.16	0.02		0.20	80.82			0.07			20.61	0.04	0.05					0.10							0.01	102.09	21.26	0.00	0.36
T3	0.26					82.29						19.04							0.35	0.05		0.05	0.06				102.10	19.81	0.16	0.26
T3	0.11					80.97						21.46		0.02					0.20								102.76	21.79	0.00	0.11
T3	0.03	0.09	0.02		0.04	80.75						21.67							0.08								102.69	21.94	0.00	0.17
T3	0.09	0.10			0.08	80.52					0.01	21.74		0.04					0.09								102.68	22.16	0.00	0.27
T3		0.08			0.06	80.41						21.18		0.02					0.06								101.79	21.39	0.00	0.13
T3	0.08	0.24	0.04		0.26	79.97			0.05			21.67	0.05	0.07		0.18			0.10							0.01	102.71	22.75	0.18	0.58
T3	0.09	0.25	0.01		0.25	79.89			0.04			21.27		0.10		0.17			0.09								102.17	22.28	0.17	0.59
T3	0.04	0.05			0.09	80.48			0.07			21.68							0.09								102.49	22.01	0.00	0.18
T3			0.08		0.03	79.21	0.16		0.17			19.14	0.14											0.04		0.02	99.00	19.78	0.00	0.03
T3	0.06	0.03	0.02		0.01	80.78			0.05			20.57		0.02					0.07								101.62	20.84	0.00	0.11
T3	0.03	0.15	0.02		0.18	80.83			0.06			21.64		0.02					0.08								103.02	22.18	0.00	0.36
T3	0.03	0.11			0.08	80.66			0.06			21.10		0.00													102.05	21.39	0.00	0.22
T3	0.04	0.15			0.22	80.84			0.04			21.66		0.03		0.14											103.12	22.27	0.14	0.41
T3	0.10	0.24	0.03		0.27	79.47			0.04			22.09	0.03	0.08					0.08							0.01	102.43	22.97	0.00	0.61
T3	0.03					76.75						21.26															98.03	21.28	0.00	0.03
T3	0.06	0.03	0.02		0.08	85.08			0.07			17.00	0.03	0.01					0.09						0.02	0.01	102.50	17.42	0.00	0.17
T3		0.16			0.10	80.56			0.05			21.07		0.01					0.07								102.02	21.46	0.00	0.26
T3	0.30					80.47						19.96							0.24					0.02	0.02		101.02	20.54	0.00	0.30
T3	0.07	0.02	0.01		0.04	79.39			0.05			21.04		0.05					0.08								100.76	21.37	0.00	0.13
T3	0.05	0.13	0.01		0.16	81.01			0.04			21.94		0.02		0.19			0.07							0.01	103.63	22.62	0.19	0.33

APPENDIX

T3	0.14	0.11			0.05	79.82			0.04			21.33		0.03					0.08								101.61	21.79	0.00	0.30
T3	0.11	0.14	0.03		0.18	79.82						21.82	0.01	0.03					0.13							0.01	102.29	22.46	0.00	0.44
T3						81.12						20.15							0.10	0.03					0.02		101.43	20.31	0.03	0.00
T3	0.33			0.02	0.04	80.43						21.33		0.09					0.14								102.37	21.94	0.00	0.37
T3	0.05	0.11			0.10	79.90			0.05			21.54		0.03					0.10							0.01	101.89	21.99	0.00	0.27
T3	0.06	0.07			0.13	80.38						21.31		0.07					0.06								102.09	21.70	0.00	0.27
T3	0.32					80.39						19.77		0.15					0.36								100.99	20.60	0.00	0.32
T3	0.20					80.43						21.14							0.15								101.92	21.49	0.00	0.20
T3	0.02	0.14	0.02		0.13	80.53					0.01	21.39		0.02					0.10								102.36	21.83	0.00	0.29
T3	0.01					80.56			0.07			21.19							0.09								101.93	21.36	0.00	0.01
T3	0.08	0.12			0.10	80.20						21.45		0.04					0.09								102.08	21.88	0.00	0.30
T3	0.06	0.18			0.13	80.37					0.01	20.65		0.04					0.10								101.53	21.17	0.00	0.37
T3	0.01	0.04			0.05	80.30						21.42							0.09								101.91	21.61	0.00	0.10
T3	0.15	0.21	0.02		0.29	79.72			0.08			21.83	0.02	0.09	0.09	0.16			0.13							0.01	102.81	23.09	0.25	0.65
T3	0.04	0.14	0.03		0.12	79.36			0.05			21.19		0.03		0.16											101.13	21.77	0.16	0.30
T3	0.04	0.11			0.12	80.25			0.05			21.25	0.03	0.04					0.12							0.01	102.02	21.77	0.00	0.27
T3		0.10	0.03		0.13	79.44			0.05			21.56		0.03												0.01	101.35	21.91	0.00	0.23
T3	0.41	2.31	0.16		2.52	73.86			0.26			25.22	0.50	0.60	1.14	1.94	1.27		0.15							0.07	110.40	36.54	4.35	5.24
T3	0.07	0.10			0.21	79.85						21.69		0.04		0.23			0.06								102.24	22.39	0.23	0.38
T3	0.10	0.09	0.01		0.14	79.54			0.04			21.59		0.06					0.11								101.70	22.15	0.00	0.34
T3	0.05	0.05				80.34			0.05			21.00		0.02					0.08				0.04				101.62	21.28	0.00	0.11
T3	0.17	0.15			0.15	79.55						21.69		0.12	0.14	0.33											102.30	22.75	0.47	0.47
T3	0.05					80.17						20.08															100.30	20.13	0.00	0.05
T4	0.07	0.08			0.06	76.48						25.18		0.01					0.13								102.00	25.52	0.00	0.20
T4	0.12					75.83						25.17							0.07								101.19	25.36	0.00	0.12
T4	0.14	0.33	0.04		0.39	75.99			0.12			25.20		0.16					0.20								102.57	26.58	0.00	0.86
T4	0.23	0.62	0.03		0.64	75.82			0.09			27.05	0.02	0.15	0.39	0.70	0.28		0.19							0.02	106.24	30.42	1.38	1.49
T4	0.07	0.10	0.02		0.20	77.17			0.08	0.01		25.37		0.03					0.20							0.01	103.28	26.11	0.00	0.37
T4						76.39						24.92							0.10								101.41	25.02	0.00	0.00
T4		0.10			0.12	78.30						23.85		0.03					0.19								102.60	24.30	0.00	0.22
T4		0.10	0.03		0.10	76.29			0.07			24.65		0.02					0.07						0.02	0.01	101.36	25.07	0.00	0.20
T4	0.04	0.23			0.20	76.07			0.05			25.83		0.04		0.12			0.13								102.72	26.64	0.12	0.47
T4			0.12	0.03		75.71	0.16		0.30	0.03	0.02	19.42	0.33					0.02	0.18				0.03		0.03	96.37	20.66	0.00	0.00
T4	0.09	0.20			0.20	76.11						26.08		0.05	0.26	0.60	0.23		0.10								103.92	27.81	1.09	0.49
T4	0.06	0.35	0.02		0.41	76.70			0.05			25.24	0.03	0.10					0.19							0.01	103.15	26.45	0.00	0.81
T4	0.10					76.67						25.13							0.18								102.08	25.41	0.00	0.10
T4	0.03	0.35	0.08		0.30	75.74			0.14			25.01	0.10	0.07					0.11							0.03	101.95	26.21	0.00	0.68
T4	0.03					76.68						25.03		0.02					0.15								101.91	25.23	0.00	0.03
T4	0.06					76.45					0.01	24.51		0.01					0.08								101.13	24.68	0.00	0.06
T4	0.08					77.08						23.77							0.22								101.15	24.07	0.00	0.08
T4	0.13	0.44	0.03		0.40	74.53			0.04			27.06		0.31	0.29	0.73	0.34		0.05								104.37	29.83	1.37	0.97
T4	0.06	0.09			0.04	76.76						25.85		0.11					0.18								103.09	26.33	0.00	0.20
T4	0.01	0.05				76.52						24.88		0.02					0.10								101.57	25.06	0.00	0.06
T4	0.12	0.16			0.21	76.18			0.05			25.48		0.05		0.15			0.18				0.02				102.59	26.41	0.15	0.49
T4	0.01	0.09	0.05		0.12	76.38			0.12		0.02	24.03	0.07	0.08					0.15				0.03		0.01		101.14	24.77	0.00	0.22
T4						76.18					0.01	24.66															100.86	24.67	0.00	0.00
T4		0.07			0.01	76.38						24.22		0.13					0.08								100.89	24.51	0.00	0.08
T4						77.18						21.20							0.16								98.54	21.37	0.00	0.00
T4	0.06	0.34	0.01		0.33	75.76						26.18		0.07	0.10	0.29			0.11								103.24	27.49	0.39	0.72

Appendix 4: Glossary of Terms (Geological) (Murdoch and Webb 1966)

Acicular: A mineral consisting of fine needle-like crystals.

Adamantine: A brilliant luster like that of a diamond.

Aggregate: A mass of rock particles, grains of minerals, or both. B. Irregular mass of crystals. C. Sand, gravel, crushed stone or rock that forms the major part of concrete.

Alkaline: Containing sodium and/or potassium in excess of the amount needed to form feldspar with the available silica. An alkaline rock, for example, contains more than average amounts of potassium- and sodium-bearing minerals.

Amorphous: Without form; applied to rocks and minerals which have no definite external crystalline structure.

Amphibole: A mineral group that consists of common, dark-colored, rock-forming silicate minerals. The most common minerals are hornblende, tremolite, and actinolite.

Andesite: A volcanic rock composed essentially of the mineral andesine and one or more of the mafic minerals.

Anhedral: Refers to a crystal with no well-formed external faces.

Arborescent: Minerals having a treelike form, with branches similar to the way a tree forms.

Asbestos: A group of naturally fibrous silicate minerals. The most common asbestos type is chrysotile.

Bed: A rock mass of large horizontal extent bounded by physically different material.

Bituminous: a. Containing much organic, or at least carbonaceous matter, mostly in the form of the tarry hydrocarbons which are usually described as bitumen. B. Pertaining to bituminous coal.

Bladed: Elongated and flattened; descriptive of some minerals.

Borates: Compounds are formed when metallic elements combine with the borate radical. Minerals include ulexite, colemanite, and howlite.

Boron mineral: Many known minerals contain boron, but only a few are commercially valuable as a source of boron. The principal boron minerals are borax, kernite, colemanite, and ulexite.

Botryoidal: A mineral surface that resembles a cluster of grapes: describes certain minerals such as hematite and malachite.

Brittle: Breaks or powders easily. A type of tenacity.

Cabochan: A style of cutting in which the top of the gemstone forms a curved convex surface. The base may be convex, concave, or flat.

Carbonaceous: a. Referring to a rock or sediment that is rich in carbon. B. Referring to a sediment containing organic matter.

Carbonates: Compounds in which one or more metallic or semimetallic elements combine with the carbonate radical. Calcite is the most common carbonate.

Chalky: Having the color, luster, or general appearance of chalk.

Chemical formula: The standard way of stating the chemical composition of a mineral in terms of the number of atoms of each element contained in that mineral.

Clastic: Consisting of fragments of minerals, rocks, or organic structures that have been moved individually from their places of origin. Synonym detrital.

Cleavable: Easily split into smaller fragments. See cleavage.

Cleavage: The property of a mineral breaking along its crystallographic planes.

Color: One of the most important properties used in determining minerals. Some minerals always show the same color, while others come in many different ones. The color of metallic (or metal-bearing) minerals is fairly constant; whereas that of non-metallic minerals is generally less so owing to the pigmentation effect of impurities. The color of a massive mineral is sometimes different from the color of its powder or streak.

Columnar: A mineral with a structure obscurely resembling prisms, for example, hornblende.

Compact: Dense crystalline texture requiring magnification to distinguish individual crystals or particles.

Conchoidal: Shell-shaped; the more compact rocks, such as flint, which break with concave and convex surfaces, are said to have a conchoidal fracture.

Concretion: A hard, compact mineral-mass of mineral matter that forms usually in sedimentary rock around a center such as bone, shell, leaf, or fossil.

Conglomerate: Refers to a cemented clastic rock containing rounded fragments of pebble size gravel; the consolidated equivalent of gravel. The composition of rock or mineral fragments may vary widely in size, but are usually rounded and smoothed from transportation by water or wave action.

Coralloidal: Having the form or appearance of coral.

Cryptocrystalline: Crystalline, but so fine-grained that the individual components cannot be seen under an ordinary microscope.

Crystal: The geometrical, faceted shape assumed naturally by minerals as they solidify, provided that nothing impedes their growth. A crystal is characterized first by its definite internal, molecular structure and second by its external form.

Crystal class: One of the 32 possible crystallographic combinations or groups of symmetry operations that leave one point, or origin, fixed. Crystal classes are divided among the six crystal systems and deal with outward symmetry.

Crystal face: The flat exterior surface of a crystal.

Crystal form: The form or shape in which crystals occur, such as the cube, the octahedron, and others.

Crystal habit: Crystal habit is a typical crystal form or a combination of forms or other shapes. It is the general shape of crystals that play an important role in identifying minerals.

Crystal system: Minerals are classified in one or more of the six designated crystal systems, according to the geometrical shapes in which minerals crystallize. These are isometric, tetragonal, hexagonal, orthorhombic, monoclinic and triclinic.

Crystalline: Made of crystal or resembling crystal. Crystalline rock is composed of crystals or fragments of crystals. Opposite ofamorphous.

Crystallography: The study of crystals, including their growth, structure, physical properties, and classification by form.

Cube: A crystal form of six equivalent and mutually perpendicular faces.

Cubic: Having the form of a cube, as a cubic crystal.

Cubo-octahedron: A crystal form which has faces of both the cube and the dodecahedron.

Dendrite: A branching figure resembling a tree produced on or in a mineral or stone by an oxide of manganese or other foreign mineral (as in the moss agate); the mineral or stone so marked.

Dendritic: Branch- and moss-like shapes or markings. For example, some crystallized native gold.

Dense: a. Compact, fine-grained, lacking pore space. B. Rock or mineral with a high specific gravity.

Deposition: Earth material of any type that has accumulated by some natural process and is large enough to invite exploration, such as a mineral or ore.

Detrital: See clastic.

Dike: A tabular body of igneous rock injected into a fissure when molten and cuts across the structure of the adjacent rocks.

Dipyramidal: A crystal form where two identical pyramids are joined base to base.

Disseminated: Fragments of minerals dispersed in a rock.

Distorted crystal: A crystal whose faces have developed unequally, some being larger than others. Some distorted crystal forms are drawn out or shortened, but the angle between the faces remains the same.

Dodecahedral: A crystal form with 12 faces. Each face (either pentagonal or rhombic) is parallel to one crystallographic axis and intersects the other two at equal distances.

Dodecahedron: An isometric form composed of 12 equal faces that are either pentagonal or rhombic.

Druse: A cavity in a rock or vein with walls encrusted with small projecting crystals.

Ductile: a. The capacity of a metal to elongate without cracking or breaking, when pulled from the ends. B. Capable of being permanently drawn out without breaking.

Dull: Those minerals in which there is a total absence of luster, as chalk or kaolin.

Earthy: Rough to the touch; dull and lusterless.

Effervesce: To bubble or hiss, as in carbonated water.

Elastic: Able to return to original shape after bending.

Element: A substance composed of atoms bearing an identical number of protons in each nucleus. An element cannot be decomposed into other substances (except by radioactive decay or bombardment with high-speed particles).

Equant: Applied to crystals having the same, or nearly the same, diameter or the same dimensions in all directions.

Evaporation: The change by which a substance is converted from a solid or liquid state into a vapor state.

Evaporites: a. One of the salts that results from the evaporation of ocean water or of saline lakes. B. Rocks such as rock salt and potash salts formed by evaporation of lakes or seas.

Face: See crystal face.

Feldspar: A mineral group that consists of abundant, light-colored, rock-forming silicate minerals. The most common minerals are microcline, orthoclase, and plagioclase.

Ferromagnesian: Containing iron and magnesium. Applied to certain dark silicate minerals, especially amphibole, pyroxene, biotite, and olivine.

Fiber: The smallest single strands of asbestos or other fibrous materials.

Fibrous: a. Applied to minerals that occur in fibers, such as asbestos. B. Consisting of fine threadlike strands; for example, satin spar.

Filiform: A mineral occurring as thin threads, often twisted like the strands of a rope; for example, native copper.

Fine: Very small in size, weight, or bulk

Flexible: Bends without breaking and will not return to its original shape.

Fluorescence: The emission of visible light by a substance exposed to ultraviolet (UV) light. Some materials, when exposed to invisible UV radiation, emit visible light and seem to "glow-in-the-dark."

Foliated: Thin, leaf-like layers of intergrowth, such as micaceous or schistose rocks.

Fracture: a. The way in which a mineral breaks, other than its cleavage. B. A crack, joint, or break in rocks.

Geode A hollow nodule or concretion, the cavity of which is commonly lined with crystals.

Glassy: Applied to igneous rocks that have no crystals, only supercooled magma. For example obsidian.

Globular: Smooth rounded surface of crystalline intergrowth.

Gossan: An iron-bearing weathered product overlying a sulfide deposit. It is formed by the oxidation of sulfides and the leaching-out of the sulfur and most metals, leaving hydrated iron oxides and rarely sulfates.

Grain: A mineral or rock particle, less than a few millimeters in diameter, and generally lacking well-developed crystal faces, for example a sand grain. Used to describe sedimentary particles of all sizes from clay to boulders, for example fine-grained and coarse-grained.

Granular: Consisting of grains of approximately equal size and ranging from two to ten millimeters.

Greasy: Applied to the luster of minerals; minerals that are oily to the touch or sight. For example talc.

Habit: The characteristic or typical crystal form, combination of forms, or other shape of a mineral, including irregularities.

Halides: Compounds in which metallic elements combine with halagens (the elements, bromine, chlorine, fluorine, and iodine). Minerals include halite and fluorite.

Hardness: Hardness is the resistance of a mineral to abrasion or scratching.

Hexagonal: One of the six crystal systems. Hexagonal crystals have four axes of symmetry; three equal horizontal axes intersect at 120 degree angles, the fourth can be either longer or shorter and perpendicular to the plane of the other three.

Hopper-shaped: Crystal faces with depressed centers because growth has been quicker along their edges than at the center.

Hydrocarbons: Organic substances that are composed only of hydrogen and carbon.

Hydrothermal veins: Veins formed at relatively high temperatures (300 degrees - 500 degrees C) and at relatively great depth.

Hydroxides: Compounds of metallic elements combined with water and hydroxyl.

Igneous: Rock formed by the solidification of molten rock (magma).

Inlier: An area or group of rocks surrounded by rocks of younger age.

Intergrowth: An interlocking of two or more minerals that resulted from their simultaneous crystallization.

Iridescent: Rainbow-like colors on the interior or surface of a mineral.

Isometric: One of the six crystal systems. Isometric crystals have three axes of equal length, all at right angles to one another.

Lamellar: Composed of thin layers, plates, or scales; disposed in layers like the leaves of a book.

Lathanides: Rare earth elements from atomic numbers 58 to 71 inclusive. They have chemical properties similar to lanthanum, a silvery-white metal that can take a high polish and which is the most common and most basic of the rare earth metals.

Lapidary: A craftsman who cuts and polishes precious stones.

Lignite: A low-grade brownish black coal.

Lode: A deposit consisting of several veins spaced closely enough so that all of them, together with the intervening rock, can be mined as a unit.

Lode gold: Gold found in veins within quartz or other rock.

Luster: The way a mineral reflects light or shines. It is one of the means for distinguishing minerals.

Mafic: Dark colored rock; usually applied to igneous and metamorphic rocks containing magnesium and iron rich minerals.

Malleable: Able to be hammered into thin sheets without breaking, as gold or silver. See tenacity.

Massive: a. A mineral deposit characterized by a great concentration of ore in one place, as opposed to a disseminated or vein deposit. B. A rock with a homogenous

texture or fabric over a wide area, with an absence of layering, foliation, cleavage, or any similar directional structure. C. Many interlocking crystals, without faces, forming masses of considerable size.

Metallic: Minerals having the luster of a metal, for example gold and copper.

Metallurgy: a. The science and art of separating metals and metallic materials from raw ore by mechanical and chemical means. B. Study of the physical properties of metals as affected by composition, mechanical working and heat treatment.

Metamorphic: Refers to rock which has been altered by heat or intense pressure at a depth in the earth's crust causing new minerals and new structures in the rock to be formed.

Mica: A group of monoclinic minerals having similar chemical compositions. The micas are prominent rock-forming constituents of igneous and metamorphic rocks.

Micaceous: Composed of or resembling mica. Occurring in thin plates or scales like mica.

Micromount: A natural mineral specimen, preferably in distinct crystals, mounted, properly labeled, and requiring magnification for meaningful observation.

Mineral: A naturally occurring inorganic substance having an orderly internal structure and characteristic chemical composition, crystal form, and physical properties.

Mineral classification: The division of minerals into classes according to aspects of their chemical composition and atomic structure.

Mineral name: A distinct mineral name is given to each mineral species. Minerals have been named after people, places, properties, and similarities with other minerals. Today, all newly discovered minerals, and their intended new name, must be presented for evaluation to the Commission on New Mineral Names of the International Mineralogical Association (IMA) so that the name is sanctioned and standardized.

Mineral species: Any mineral that can be distinguished from all other minerals. It must differ from every other mineral species either in its chemical composition or atomic structure.

Monoclinic: One of the six crystal systems. Monoclinic crystals have three unequal axes, two of which are at right angles to one another and lie in a plane, the third is inclined to the plane of the other two.

Native Occurring in nature, either pure or uncombined with other substances. Usually applied to metals, such as native mercury and native copper.

Native element: Uncombined elements that are classified into three groups: metals such as gold, semimetals such as antimony, and nonmetals such as sulfur.

Nitrates: Compounds in which one or more metallic elements combine with the nitrate radical, for example, nitratine.

Nodule: A small rounded lump of a mineral or aggregate, normally without internal structure, and having a contrasting composition from the enclosing sediment or rock in which it is embedded. For example, pyrite in a coal bed.

Nugget: A lump of native gold, silver, platinum, copper, etc.

Octahedral: Referring to or resembling an octohedron, a crystal form consisting of eight triangular faces each having equal intercepts on all three crystallographic axes.

Oily: Poorly reflective luster, similar in appearance to oil.

Oolitic: Concentric globular deposits smaller than the size of a pea.

Ore: a. Rocks or minerals that can be mined for a profit. B. The mineral(s) thus extracted.

Orthorhombic: One of the six crystal systems. Orthorhombic crystals have three unequal axes, all lying at right angles with respect to one another.

Outcrop: The part of a rock formation that appears at the ground's surface.

Overburden: A material that readily yields oxygen or other oxidizing substances needed for an explosive reaction to take place.

Pearly: Minerals with a luster like a pearl, such as talc.

Pegmatite: Coarse-grained igneous rock found usually as dikes associated with a large mass of finer grained plutonic rock.

Pentagonal: A polygon with five sides and five interior angles.

Petrify: To become stone. Organic substances such as shells, stones, and wood embedded in sediments become converted into stone by the gradual replacement of their tissues, particle by particle, with corresponding amounts of infiltrated mineral matter.

Phosphates: Compounds in which metallic elements combine with the phosphate radical. Minerals include lazulite, pyromorphite, and ludlamite.

Phosphorescence: Where a mineral continues to glow for an interval after the ultraviolet light source has been turned off. Seefluorescence.

Plagioclase: A group of minerals containing a mixture of sodium and calcium feldspar.

Platy: Mineral habit with flat, thin crystals.

Plumose: Having a feathery appearance.

Plutonic: A general name pertaining to igneous rocks formed at great depths.

Porcelaneous: Dull, white luster resembling unglazed porcelain.

Porous: Contains voids, pores, cells, and other openings that may or may not interconnect.

Prism: A crystal form with three or more similar faces parallel to a single axis.

Property: One of the physical or chemical characteristics of a material.

Pulverulent: Easily reduced to powder.

Pyramidal: A crystal form which has three, four, six, eight, or twelve nonparallel faces that meet at a point.

Pyritohedron: An isometric closed crystal form of 12 faces, each having an irregular pentagon. It is named after pyrite, which characteristically has this crystal form.

Pyroxene: This mineral group consists of common, dark-colored, rock-forming silicate minerals. The most common minerals are diopside and augite.

Radiated: Crystal aggregates that radiate from a center without producing star-like forms.

Rare earths: a. Oxides of a series of 15 metallic elements, from lanthanum (atomic number 57) to lutetium (71), and of two other elements, yttrium (39) and scandium (21). B. Rare earths are not especially rare in the earth's crust, but economic concentrations are. The rare earth metals resemble one another very closely in chemical and physical properties so it is difficult to separate them.

Reniform: A term meaning kidney-shaped, used to describe rounded mineral surfaces.

Resinous: Having the luster of resin.

Reticulated: A mineral with cross meshes, like a net.

Rhombic: Shaped liked a rhombus (an equilateral parallelogram).

Rhombohedral: Referring to a rhombohedron, which is a common crystal form in the hexagonal crystal system. Its 3-dimensional shape can be visualized as a cube stretched or compressed in the direction of two opposite corners.

Rock: An aggregate of one or more minerals, (such as granite, shale, marble) or a body of undifferentiated mineral matter, (such as obsidian) or a solid organic material, (such as coal). Rocks fall into three broadly defined groups: igneous, sedimentary, and metamorphic rocks. In some instances a single mineral forms a rock, as calcite, serpentine, and kaolin. Rock-forming

Minerals: Mineral that is common and abundant in the earth's crust; one making up large masses of rock.

Rosette: Intergrowth of numerous platy crystals overlapping like the petals of a rose.

Scaly: Consisting of scales or tabular crystals.

Schistose: Resembling schist (a crystalline rock that can be readily split or cleaved because of having a foliated or parallel structure).

Sectile: Capable of being cut with a knife into thin shavings.

Sedimentary: Pertaining to rocks formed by the sediment deposition (fragments of rocks, minerals, animal or plant material).

Series: Any number of rocks, minerals, or fossils having characteristics, such as growth patterns, succession, composition, or occurrence, that make it possible to arrange them in a natural sequence.

Serpentine: A group of common rock-forming minerals with a greasy or silky luster, a somewhat soapy feel, and a tough, conchoidal fracture. They are usually green, greenish yellow or greenish gray and often veined or spotted with green and white.

Sheen: The way a mineral reflects light can be affected by characteristics just below the mineral's surface: for example, the pearly sheen caused by partly-developed cleavage(s) parallel to the surface; the silky sheen from a fibrous growth structure or parallel hair-like inclusions.

Silica: A dioxide of silicon, which occurs in crystalline form as quartz, crystobalite, amorphous opal; an essential constituent of the silicate group of minerals.

Silicates: Compounds in which metallic elements combine with either single or linked Si-O tetrahedra. Stucturally, minerals in this class are subdivided according to their crystalline structure, into various groups (for example, ring silicates, single-chain silicates, framework silicates) rather than their chemical formula. Minerals include beryl, tourmaline, and epidote.

Silky: Having the luster of silk.

Skeletal: In crystallography, hollow or imperfectly developed crystals formed by rapid crystallization.

Soluble: Capable of being dissolved in a fluid.

Spalling: The chipping and upward and outward heaving of rock caused by release of pressure.

Specific gravity: The ratio of a specimen's weight compared with the weight of an equal volume of water. Therefore, if the weight of a mineral specimen is three times that of the volume of water it displaces, its specific gravity is three.

Specimen: A sample, as of a mineral, rock, ore, or fossil.

Spherulitic: A rounded mass of acicular crystals, radiating from a central point.

Splintery: The property of certain minerals or rocks to break or fracture into elongated fragments like splinters of wood.

Spongy: Applied to vesicular rock structures with thin partitions between the vesicles, thus resembling a sponge.

Stalactitic: Like a stalactite, a conical or cylindrical mineral deposit that hangs from the ceiling of a cave.

Stellate: An aggregate of crystals in starlike arrangement.

Streak: A mineral's powder color. It is most easily observed by rubbing the mineral on a piece of white unglazed porcelain (called a streak plate). Also, streak can be observed by fine crushing a specimen with a hammer.

Subvitreous: Luster not as highly reflective as adamantine, but more so than vitreous.

Sulfates: Compounds in which one or more metallic elements combine with the sulfate radical. Minerals include barite, gypsum, and linarite.

Sulfides: Compounds in which sulfur combines with metallic and semimetallic elements. Minerals include cinnabar, pyrite, and galena.

Sulfosalts: Compounds in which metallic elements combine with sulfur plus a semimetallic element, for example, stephanite.

Tabular: Crystal habit with the appearance of a paper tablet.

Tenacity: The strength of a mineral; its resistance to breaking, crushing, bending, or tearing. Terms commonly used to describe the tenacity of a mineral are brittle, sectile, malleable, flexible, elastic, ductile, and tough.

Tetragonal: One of the six crystal systems. Tetragonal crystals have three axes at right angles of which only two lateral axes are equal.

Tetrahexahedron: A crystal form of the isometric system, bounded by twenty-four equal triangular faces, four to each face of the cube.

Tough: Strong and firm in texture but flexible and not brittle; capable of resisting great strain without coming apart.

Triclinic: One of the six crystal systems. Triclinic crystals share three axes, all having different lengths and perpendicular to the others.

Trisoctahedron: A form with 24 congruent triangular faces and having an octahedron base.

Tufted: Refers to a crystal aggregate in the form of fibrous crystal clumps.

Tungstates: Compounds in which metallic elements combine with the tungstate radical. Minerals include scheelite and wolframite.

Twin crystal: Two portions of a crystal having a definite crystallographic relationship.

Twinning: An intergrowth of two or more single crystals of the same substance.

Vanadates: Compounds in which metallic elements combine with the vanadate radical, for example, carnotite.

Variety: A mineral showing differences in color, other physical properties, or minor variations in composition from the typical species material. For example, amethyst is the purple variety of the mineral species quartz which has many other varieties as well.

Vein: A zone or belt of mineralized rock lying within boundaries clearly separating it from neighboring rock. It includes all deposits of mineral matter found through a mineralized zone or belt coming from the same source, impressed by the same forms, and appearing to have been created by the same method.

Veinlet: a small vein.

Vesicle: A small cavity in a glassy, igneous rock formed by the expansion of a gas bubble or steam during the solidification of the rock.

Vitreous: Luster similar to freshly broken glass; brightly reflective.

Wad: A dark brown or black, impure mixture of manganese and other oxides. It contains 10 to 20 percent water, and is generally soft; massive and of low specific gravity. Also called black ocher; earthy manganese; bog manganese.

Waxy: Mineral luster that is only slightly reflective; typical of minutely granular surfaces.

Wiry: A mineral occurring as thin wires, often twisted like the strands of a rope, for example native copper.

Appendix 5: Glossary of Terms (General)

Platinum Group Elements (PGEs) PGEs are a specific group of noble metals that display similar chemical and physical characteristics to one another. They include: platinum (Pt), palladium (Pd), osmium (Os), ruthenium (Ru), rhodium (Rh) and iridium (Ir). However, PGEs have a strong affinity towards arsenic (As), sulphur (S), selenium (Se) and tellurium (Te) which result in complex mineralogy. So far, 144 minerals of PGE were identified (Smith and Nickel 2007).

Rim Formation Simplification:

1. Biological: Bacterial Biofilms associated with the Ralstonia *metallidurans* show an aerated network of budding spherical particles as small as 3 µm (Reith et al. 2006).
2. Dealloying: Selective corrosion of one or more components of a solid solution alloy.
3. Mechanical strain: Change in shape, or non-rigid body deformation of a rock caused by stresses.

EDS: **Energy Dispersive X-ray Spectroscopy (EDS, EDX or XEDS)** A qualitative and quantitative X-ray microanalytical technique that can provide information on the chemical composition of a sample for elements with atomic number (Z) >3.

EPMA: **Electron probe micro-analyser** An electron probe micro-analyser is a microbeam instrument used primarily for the *in situ* non-destructive chemical analysis of minute solid samples. EPMA is also informally called an electron microprobe, or just probe. It is fundamentally the same as an SEM, with the added capability of chemical analysis. The primary importance of an EPMA is the ability to acquire precise, quantitative elemental analyses at very small "spot" sizes (as little as 1-2 microns), primarily by wavelength-dispersive spectroscopy (WDS).

FFT: **Fast Fourier Transform**: An algorithm that computes the discrete Fourier transform (DFT) of a sequence, or its inverse (IFFT). Fourier analysis converts a signal from its original domain (often time or space) to a representation in the frequency domain and vice versa. An FFT rapidly

computes such transformations by factorizing the DFT matrix into a product of sparse (mostly zero) factors.

FIB: **Focussed Ion Beam**: Uses a finely focused beam of ions (usually gallium) that can be operated at low beam currents for imaging or at high beam currents for site specific sputtering or milling.

HAADF-STEM: **High-angle Annular Dark-field Scanning Transmission Electron Microscopy** High-angle annular dark-field scanning transmission electron microscopy (HAADF-STEM) is a STEM method which receives inelastically scattered electrons or thermal diffuse scattering (TDS) at high angles using an annular dark-field (ADF) detector (～50 to sufficiently high angle; e.g. ～200 mrad).

Kikuchi lines: Kikuchi lines pair up to form bands in electron diffraction from single crystal specimens, there to serve as "roads in orientation-space" for microscopists not certain at what they are looking. In transmission electron microscopes, they are easily seen in diffraction from regions of the specimen thick enough for multiple scattering.[1] Unlike diffraction spots, which blink on and off as one tilts the crystal, Kikuchi bands mark orientation space with well-defined intersections (called zones or poles) as well as paths connecting one intersection to the next.

SEM: **Scanning Electron Microscopy** The signals used by a scanning electron microscope to produce an image result from interactions of the electron beam with atoms at various depths within the sample. Various types of signals are produced including secondary electrons (SE), reflected or back-scattered electrons (BSE), characteristic X-rays and light (cathodoluminescence) (CL), absorbed current (specimen current) and transmitted electrons.

TEM: **Transmission Electron Microscopy** A microscopy technique in which a beam of electrons is transmitted through a specimen to form an image. The specimen is most often an ultrathin section less than 100 nm thick or a suspension on a grid. An image is formed from the interaction of the electrons with the sample as the beam is transmitted through the specimen. The image is then magnified and focused onto an imaging device, such as a fluorescent screen, a layer of photographic film, or a sensor such as a charge-coupled device.